From hydraulic root architecture models to macroscopic representations of root hydraulics in soil water flow and land surface models.

Jan Vanderborght[1], Valentin Couvreur[2], Felicien Meunier[3,4], Andrea Schnepf[1], Harry Vereecken[1], Martin Bouda[2,5], and Mathieu Javaux[1,2].

[1] Forschungszentrum Jülich GmbH, IBG-3 (Agrosphäre), Wilhelm-Johnen-Str., 52428 Jülich, Germany.

[2] University of Louvain, Earth and Life Institute, 1348 Louvain-la-Neuve, Belgium

[3] CAVElab - Computational and Applied Vegetation Ecology, Department of Environment, Ghent University, Ghent, Belgium

[4] Department of Earth and Environment, Boston University, Boston, USA

[5] Institute of Botany of the Czech Academy of Sciences, Pruhonice, Czechia

Correspondence to: Jan Vanderborght (j.vanderborght@fz-juelich.de)

Abstract: Root water uptake is an important process in the terrestrial water cycle. How this process depends on soil water content, root distributions, and root properties is a soil-root hydraulic problem. We compare different approaches to implement root hydraulics in macroscopic soil water flow and land surface models. By upscaling a three dimensional hydraulic root architecture model, we derived an exact macroscopic root hydraulic model. The macroscopic model uses three characteristics: the root system conductance, K_{rs}, the standard uptake fraction, **SUF**, that represents the uptake from a soil profile with a uniform hydraulic head, and a compensatory matrix that describes the redistribution of water uptake in a non-uniform hydraulic head profile. Two characteristics, K_{rs} and **SUF**, are sufficient to describe the total uptake as a function of the collar and soil water potential; and water uptake redistribution does not depend on the total uptake or collar water potential. We compared the exact model with two hydraulic root models that make a-priori simplifications of the hydraulic root architecture: the parallel and big root model. The parallel root model uses only two characteristics, K_{rs} and **SUF,** that can be calculated directly following a bottom-up approach from the 3D hydraulic root architecture. The big root model uses more parameters than the parallel root model but these parameters cannot be obtained straightforwardly with a bottom-up approach. The big root model was parameterized using a top-down approach, i.e. directly from root segment hydraulic properties assuming a-priori a single big root architecture. This simplification of the hydraulic root architecture led to less accurate descriptions of root water uptake than by the parallel root model. To compute root water uptake in macroscopic soil water flow and land surface models, we recommend the use of the parallel root model with K_{rs} and **SUF** computed in a bottom-up approach from a known 3D root hydraulic architecture.

1 Introduction

Plant transpiration, which corresponds with about 40% of the precipitation on land (Oki and Kanae, 2006;Trenberth et al., 2007;Good et al., 2015) is an important component of the terrestrial water cycle. It drives water flow from the soil into the plant and plays an important physiological role for distributing minerals from the soil to the above ground part of the plant and for regulating the temperature of the leaves. Understanding where and when plants take up water from the soil is important to unravel the interaction between climate, soil and plant growth, manage soil water, and select or breed plants that are optimally performing in a certain soil-climate environment. Therefore, root water uptake is a sensitive process in land surface and crop models (Gayler et al., 2013;Wöhling et al., 2013;Vereecken et al., 2015;Ferguson et al., 2016;Vereecken et al., 2016;Whitley et al., 2017).

There are several ways to distinguish and classify root water uptake models: macroscopic versus microscopic, mechanistic versus empirical, and bottom-up versus top-down (Feddes et al., 2001;Hopmans and Bristow, 2002). Here, we will focus on models that describe water flow in the soil-root system mechanistically based on soil and plant hydraulics, i.e. based on water potential gradients in each system, on root and soil conductances, and on exchange or radial soil-root conductances. When water flow is described mechanistically in the soil-plant system, processes with an important impact on root water uptake emerge from the model simulations and do not have to be parameterized (Javaux et al., 2013). These include hydraulic redistribution when water uptake from the wetter part of the root zone is released in the drier part and root water uptake compensation when root water uptake shifts to wetter zones (Katul and Siqueira, 2010). The differences between different modeling approaches that we consider are related to the spatial representation of the root system and its architecture or topology.

A first approach to model this system is to start with a simplified concept of the root system or its topology. Although the topology of the root system may also be considered as a parameterization of a model that describes water flow in the soil root system, we consider the root topology here as specific 'model' that is fixed a-priori in a kind of top-down approach and that is subsequently parameterized based on measurements of soil water potential, leaf water potential, transpiration fluxes and information about the root system such as the root density distribution and hydraulic properties of root segments. Two a-priori proposed root system topologies can be distinguished: big root and parallel root models.

Big root models are 1D models in which the root system is represented by one vertical 'big root'. In this model, all root segments in a layer at a certain depth are grouped in one 'tube' and these tubes are connected in series with each other. Nimah and Hanks (1973) used this approach for simulating root water uptake but simplified the head losses due to axial flow. The axial big-root hydraulic conductance, which determines head losses due to axial flow in the root system, and the radial big-root conductance, which determines the exchange between the soil and the root, were obtained by scaling intrinsic root segment conductances with the cross sectional and surface area of the root segments in the soil profile, respectively; and the unsaturated soil hydraulic conductivity (Amenu and Kumar, 2008;Quijano and Kumar, 2015).

The second simplified root topology model is what we define as the 'parallel root model'. In the 'parallel root model', the root system is conceptualized to consist of branches of different lengths that take up water near their tips and that are all connected in parallel to a root collar node (Gou and Miller, 2014). The parallel root system considers a connection in series between the radial and axial conductances of a single root branch. Thus, this model can also account for axial root conductances or for head losses due to flow along the root branch (Hillel et al., 1976). The model is parameterized by the distribution of absorbing root surface with depth and the conductances of the root branches that connect these surfaces with the root collar. Although it is not identical to the parallel root model, a model that shows similarities with the parallel root model is the model by Ryel et al. (2002) which has been implemented in several land surface models.

A further simplification is to neglect the axial resistance so that the water potential in the root xylem is everywhere the same (Gardner and Ehlig, 1962;Wilderotter, 2003;de Jong van Lier et al., 2008;Siqueira et al., 2008;de Jong van Lier et al., 2013;Manoli et al., 2014;Daly et al., 2018). This simplification wipes out the difference between the 'big root' and 'parallel root' models.

The second approach starts from an explicit 3D representation of the root architecture and the distribution of root segment conductances and describes the flow in the branched root network that is coupled to flow in the soil (Doussan et al., 1998;Doussan et al., 2006;Javaux et al., 2008). Hydraulic characteristics of the root system such as the root system conductance and the root water uptake distribution for a uniform soil water potential distribution can be derived using analytical solutions of the flow equations in the root system. These characteristics were derived for single roots with constant (Landsberg and Fowkes, 1978) or with varying root hydraulic properties (Meunier et al., 2017b), and for branched root systems (Roose and Fowler, 2004;Meunier et al., 2017c). The solutions provide a direct or a bottom-up link between the root architecture and the hydraulic properties of root segments on the one hand and the hydraulic root system characteristics on the other hand (Meunier

et al., 2017a). By making assumptions about the axial conductance of the root system, Couvreur et al. (2012) derived an approximate model that simulates the uptake for arbitrary soil water potential distributions within the root zone and that uses these hydraulic root system characteristics. The form of the obtained model is similar to that of the parallel root model but it uses root system characteristics that were derived from an exact or numerical solution of the flow in the 3D hydraulic root architecture. In other words, even though the model formulation is similar to the parallel root model, the systems' properties were not derived in a top-down approach by a-priori assuming a parallel root model. The model was formulated originally to simulate the 3D distribution of the water uptake in the soil by a 3D root architecture. When it is assumed that the soil water potentials do not vary in the horizontal direction, the model can be scaled up to a 1D formulation of the same form to calculate vertical water uptake profiles (Javaux et al., 2013;Couvreur et al., 2014a). Another approach was followed by Bouda and Saiers (2017) who derived an upscaled 1D root water uptake model using a so-called root system architecture stencil that is calibrated on solutions of water flow in a 3D root architecture. Bouda (2019) showed recently that the root system architecture stencil they derived based on solutions of water flow in 3D root system architectures is similar to an analytically exact solution of the big root model.

Both big root and parallel root models are approximations of the real 3D root architecture and the connectivity of the individual root segments and topology of the root system may have an important impact on the root system functioning (Bouda et al., 2018). Analytical solutions of water uptake by single roots, which are represented as 'porous pipes' with uniform radial and axial conductances, demonstrated that water uptake takes place along the entire root length but that due to limiting axial conductance, uptake may decrease from the proximal to the distal part of roots (Landsberg and Fowkes, 1978). The solutions obtained with these models question assumptions made in parallel root models about negligible axial root resistances or about negligible uptake along the root and suggest that a big root model may be a better option. On the other hand, root tissue maturation generally leads to a decrease of radial root conductivity towards the older proximal end of roots so that root water absorbance can be larger near the root tips. A fibrous root system architecture with several lateral roots that are connected at the root collar and that take up water near the root tips might be represented better by a parallel root model than by a big root model, even when axial resistances cannot be neglected. In case of several parallel root branches, the xylem water potentials may differ between the different branches at a given depth and a big root model is not able to account for these variations in xylem water potentials.

Upscaling of water flow in 3D root architectures to models that describe 1D root water uptake profiles in soils is crucial to implement root hydraulics in land surface models that describe exchanges of water and energy between the land surface and the atmosphere at catchment, continental and global scales. Also for crop models, which predict crop growth and yield at the field scale, an upscaling to 1-D uptake profiles is necessary. Root hydraulics has been implemented in 1D land surface models using big root or parallel root models to represent emerging processes like hydraulic redistribution and root water uptake compensation, which have an important impact on transpiration, assimilation and biogeochemical cycles during dry spells and seasons (Quijano et al., 2013;Liu et al., 2020). Yan and Dickinson (2014) and Fu et al. (2016) implemented the parallel root like model of Ryel whereas Tang et al. (2015) implemented a big root model. Kennedy et al. (2019) implemented a parallel root model in CLM and Sulis et al. (2019) implemented an approach proposed by Couvreur et al. (2012), which is for a certain parameterization equivalent to a parallel root model. Nguyen et al. (2020) demonstrated that differences in drought stress and crop growth in different soils with different soil hydraulic properties could be predicted by a crop model that considers root hydraulics whereas commonly used empirical relations failed. Root hydraulics are also important to describe the interaction of different species that share the same soil volume. Quijano et al. (2012) developed a multispecies model that simulates root water uptake by different species from a shared soil water reservoir based on their big root model. Each species was represented by its own big root model and the different big root models took up water from the shared soil water profile. The model demonstrated the impact of hydraulic redistribution on the uptake by the different species and their mutualistic dependencies. Water taken up deep in the soil profile by deep rooting trees was released in the shallower soil layers where it could be accessed

by shrubs or understory vegetation. Similar conclusions were drawn by Manoli et al. (2014) and Manoli et al. (2017) using a parallel root system model. Although all models reproduced the impact of root hydraulics on ecosystems fluxes, a model comparison by Zhu et al. (2017), who compared Ryel's model with a big root model and an empirical root water uptake compensation model, highlighted that different models led to fairly different results. However, the nature of these differences is not well understood.

The objective of this paper is to derive with a bottom-up approach an exact upscaled 1D model that describes root water uptake considering the hydraulics of the 3D root architecture and that could readily be implemented in land surface models. The model will be compared with parallel root and big root models that are currently used in 1D models. In order to interpret the models and their differences, we will cast in a first part the solutions of the models in a form that uses two hydraulic root system characteristics: the root system conductance and the root water uptake distribution for a uniform soil water potential or hydraulic head distribution. This was already done for a parallel root system by Couvreur et al. (2012) but an exact formulation of root water uptake in terms of these characteristics for a general root system model, including a 3D root model and its upscaled version and a big root model, is still missing. We will show that these characteristics are for all models sufficient to describe the total root water uptake as a function of soil and collar water potentials or hydraulic heads. We will further show that these root system characteristics fully define the parallel root model. Additional terms or factors in the equation for the exact root system can be used as diagnostics of the deviation between the parallel root system model and the exact 3D model or its upscaled version due to differences in root system topology. A second consequence of the parallel root model being fully defined by the two root hydraulic characteristics is that it can be parameterized straightforwardly in a bottom-up approach. In a second part, we will compare the upscaled exact model with the parallel and big root models that can be parameterized in two different ways: a top-down parameterization in which parameters are derived from the root segment distribution and root segment hydraulic parameters assuming a-priori big root or parallel root topologies, versus a bottom-up parameterization of the parallel root model that uses exact hydraulic root system characteristics obtained from solving the flow equations in the 3D hydraulic root architecture (Figure 1). For the parallel root system model, we can evaluate to what extent the simulated uptake is impacted by the simplified root system topology while using exact hydraulic root system characteristics. First, the models will be compared for a very simple hypothetical root system that represents a hybrid form of the two 'asymptotic' root architectures (parallel root versus big root model). Second, the models will be compared for single roots with realistic distributions of root segment properties and for realistic root architectures of plants with a tap root or a fibrous root system.

50
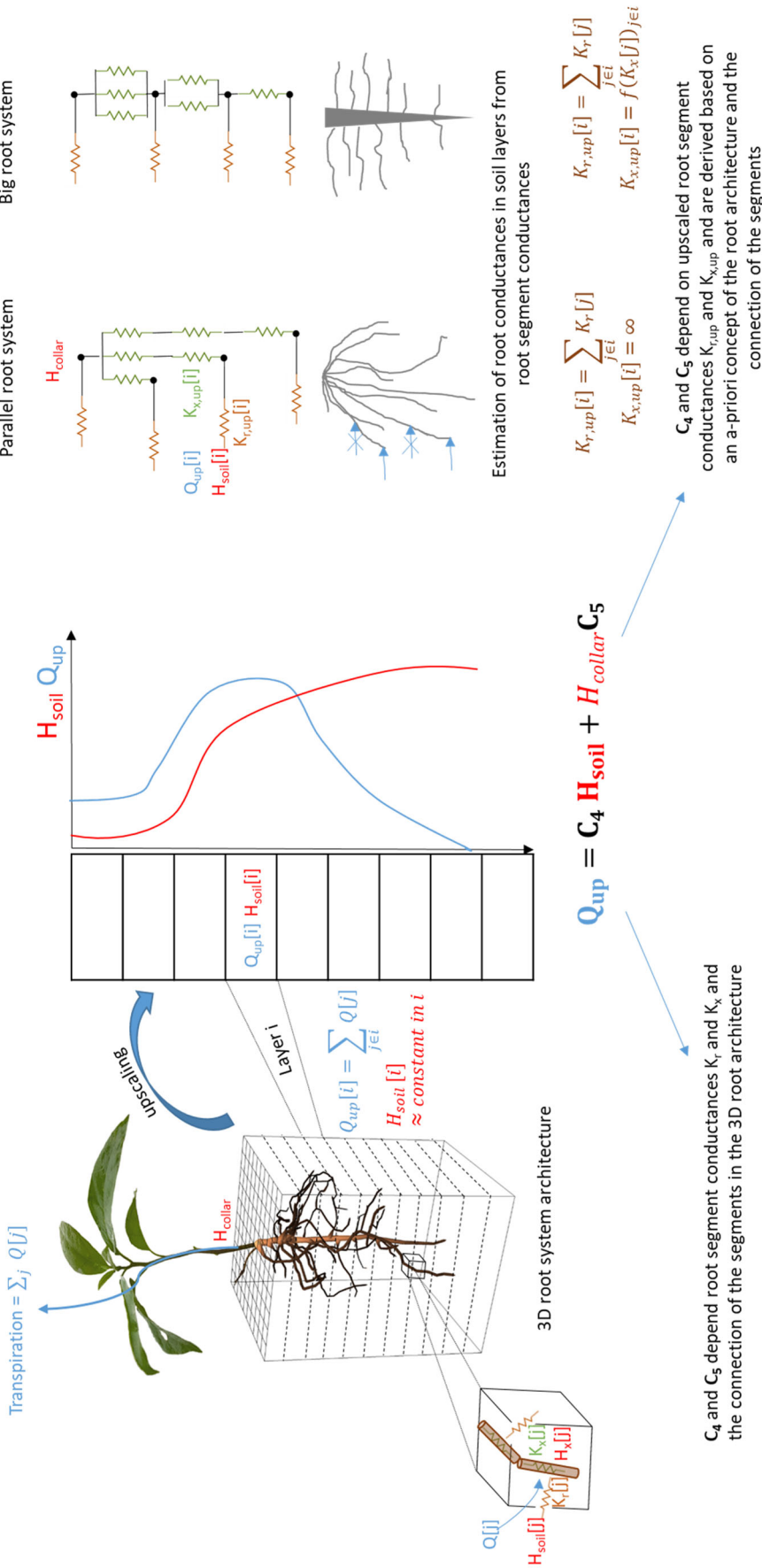
51 **Figure 1: Bottom-up approach versus top-down approaches for a parallel and a big root system model to derive and parameterize**
52 **an upscaled one dimensional root water uptake model.**

2   Set up of equations

155   The flow into and within a single root can be described using the porous pipe model (Landsberg and Fowkes, 1978) with the following equation:

$$\frac{d}{d\ell} k_x \frac{dH_x}{d\ell} = -2\pi r k_r \left(H_{soil} - H_x \right) \tag{1}$$

where ℓ [L] is the local axial coordinate of the root, k_x (L^3 T^{-1}) and k_r (T^{-1}) are the intrinsic axial and radial root segment conductances, r [L] is the root segment radius, and H_x (L) and H_{soil} (L) are the hydraulic heads of the water in, respectively, the xylem and the soil in contact with the root, which include both the pressure potential and the elevation potential. Intrinsic

160   conductances refer here to properties of the root segments that are independent of the axial discretization that we use to solve the equation. We can discretize this equation for a root system network that consists of N_{root} root segments (edges) that are connected with each other in nodes (vertices). The entire network is connected to one outlet node that represents the root collar where the hydraulic head, H_{collar}, or the flux boundary condition is defined. Since branches of a root architecture do not re-join distally (further away from the collar), there is only one segment that connects a certain node with the proximal (closer to the

165   collar) part of the root system or each node is the distal node of only one element (except for the collar node). Therefore, the network of N_{root} root segments connects N_{root} root nodes with each other and the root collar. The root nodes (but not the collar node), are connected by N_{root} soil-root segments to N_{root} soil nodes. The total number of segments (root segments connecting root nodes and soil-root segments connecting root with soil nodes) is $2N_{root}$. The total number of nodes in this system, including the collar node, is $2N_{root}+1$. Each root node (except the collar node) can be linked uniquely to two segments: a root segment

170   that connects the node to the proximal part of the root system and a soil-root segment that connects the node to the soil. The axial conductance $K_x[i]$ (L^2 T^{-1}) of the proximal root segment and the radial conductance of the soil-root segment $K_r[i]$ (L^2 T^{-1}) connected to the ith root node are defined as:

$$K_x[i] = \frac{k_x[i]}{l[i]} \tag{2}$$

$$K_r[i] = 2\pi r[i] l[i] k_r[i] \tag{3}$$

where $l[i]$ (L) is the length and $r[i]$ (L) the radius of the proximal root segment connected to the ith root node. The transpiration stream to the collar, T (L^3 T^{-1}), the xylem hydraulic heads, and the fluxes from the soil to the root nodes Q (L^3

175   T^{-1}) are obtained from solving the Laplacian matrix of the weighted directed graph of soil and root nodes, which is the discrete representation of the flow equation in the porous pipe root system:

$$\left[\mathbf{IM} \cdot diag(\mathbf{K}) \cdot \mathbf{IM^T} \right] \begin{bmatrix} H_{collar} \\ \mathbf{H_x} \\ \mathbf{H_{soil}} \end{bmatrix} = \begin{bmatrix} -T \\ \mathbf{0} \\ \mathbf{Q} \end{bmatrix} \tag{4}$$

where $\mathbf{IM}$ is the ($2N_{root}+1$ x $2N_{root}$) incidence matrix of the graph with $2N_{root}+1$ nodes and $2N_{root}$ segments. The rows of the incidence matrix represent the nodes of the graph and the columns the segments. The first row represents the root collar, the next N_{root} rows the root nodes and the last N_{root} rows the soil nodes. The first N_{root} columns represent the root segments and the

180   last N_{root} columns soil-root elements. $IM[i,j]=1$ when node i is a distal node of element j, $IM[i,j] = -1$ when i is proximal node of element j and $IM[i,j]=0$ otherwise. $\mathbf{H_x}$ is the N_{root} vector with xylem hydraulic heads in the root nodes and $\mathbf{H_{soil}}$ the N_{root} vector with the soil water hydraulic heads in the soil nodes. diag($\mathbf{K}$) is a diagonal conductivity matrix with the first N_{root} diagonal elements representing the xylem conductivities and the last N_{root} elements the radial conductances. $\mathbf{0}$ is an N_{root} vector with zeros and $\mathbf{Q}$ is the N_{root} vector with fluxes from the soil nodes to the root nodes. The derivation of Eq. [4] is demonstrated

in the appendix. The first equation represents the total transpiration stream out of the network as a function of the hydraulic heads in the root collar and the root nodes connected to the collar and the axial conductances of the root segments connected to the root collar. The next N_{root} equations close the water balances in root nodes and from solving these, the xylem hydraulic heads in the root nodes are obtained. The last N_{root} equations yield the fluxes Q from the soil nodes to the root nodes. Plugging the obtained xylem hydraulic heads in the last N_{root} equations, the fluxes towards each root node are obtained from Eq. [4] (see Appendix) as:

$$\mathbf{C_4 H_{soil}} + \mathbf{C_5} H_{collar} = \mathbf{Q} \qquad [5]$$

where $\mathbf{C_4}$ ($L^2\ T^{-1}$) is an N_{root} x N_{root} symmetric matrix and $\mathbf{C_5}$ ($L^2\ T^{-1}$) an N_{root} x 1 column. The relations between $\mathbf{C_4}$, $\mathbf{C_5}$, the root segment conductivities (stored in diag($\mathbf{K}$)) and the segment connections (defined in the incidence matrix $\mathbf{IM}$) are given in Table 1. This equation can be written in another form that uses macroscopic characteristics of the root system: the root system conductance, K_{rs} ($L^2\ T^{-1}$), and the standard uptake fraction vector $\mathbf{SUF}$ (N_{root}x1) of the root nodes that were introduced by Couvreur et al. (2012). K_{rs} relates the total root water uptake to the difference between an average or effective soil water hydraulic head, H_{eff} (L) and H_{collar}:

$$T = \sum_i \mathbf{Q} = K_{rs} \left(H_{eff} - H_{collar} \right) \qquad [6]$$

$SUF[i]$ represents the fraction of the total uptake by the ith root node for a uniform H_{soil}. In the appendix, we derive that H_{eff} corresponds with the SUF-weighted average of H_{soil}:

$$H_{eff} = \mathbf{SUF}^T \mathbf{H_{soil}} \qquad [7]$$

Eq. [7] implies that the effective soil water hydraulic head depends more strongly on soil water hydraulic heads where the root system takes up more water when the soil water hydraulic head is uniform. Eqs. [6] and [7] imply that K_{rs} and $\mathbf{SUF}$ are sufficient root system properties to calculate the total root water uptake. Using these macroscopic root system characteristics, Eq. [5] can be rewritten as:

$$\mathbf{Q} = K_{rs} \mathbf{SUF} \left(H_{eff} - H_{collar} \right) + \mathbf{C_4} \left(\mathbf{H_{soil}} - \mathbf{H_{eff}} \right) \qquad [8]$$

where $\mathbf{H_{eff}}$ is a (N_{root}x1) vector filled with H_{eff}. The derivation of Eq. [8] is given in the appendix and we summarize the main properties of the equation here. The first term on the right-hand side of Eq. [8] represents the uptake from the soil profile when the soil water hydraulic head is uniform and equal to H_{eff}. The definition of H_{eff} as the SUF-weighted average of H_{soil} makes that the sum of the fluxes of the second term of the right hand side of Eq. [8] becomes zero (see Eq. [A 33]). The second term on the right-hand side represents the increase (decrease) in amount of water that is taken up by a root node that is connected to soil node where H_{soil} is higher (lower) than H_{eff}. This second term represents the compensatory uptake and we name the $\mathbf{C_4}$ matrix the compensatory matrix. Of note is that the second term only depends on the hydraulic root architecture (defining $\mathbf{C_4}$ and $\mathbf{SUF}$) and on the soil water hydraulic head distribution. It neither depends on the water potential at the root collar nor on the transpiration rate. As a consequence, root water uptake compensation changes over time only due to changes in the soil water hydraulic heads but not due to e.g. diurnal changes in transpiration rate. In Table 1, relations between K_{rs}, $\mathbf{SUF}$, $\mathbf{C_4}$, H_{eff} and the root hydraulic architecture are given.

Table 1: Equations to calculate the root system hydraulic conductance, K_{rs}, the standard uptake fraction, SUF, the compensatory uptake matrix, C_4, from the hydraulic root architecture.

$\mathbf{C} = \mathbf{IM} \cdot diag(\mathbf{K}) \cdot \mathbf{IM}_{\mathbf{collar}}^{\mathbf{T}} \quad (2N_{root}+1 \text{ x } 2N_{root}+1)$	[9]
$\mathbf{C_1} = C[i,j] \text{ for } i=2,...,N_{root}+1, j=1$	[10]
$\mathbf{C_2} = C[i,j] \text{ for } i=2,...,N_{root}+1, j=2,...,N_{root}+1$	[11]
$\mathbf{C_3} = C[i,j] \text{ for } i=2,...,N_{root}+1, j=N_{root}+2,...,2N_{root}+1$	[12]
$\mathbf{C_4} = diag(\mathbf{K_r})\left[\mathbf{I} + \mathbf{C_2}^{-1}\mathbf{C_3}\right] \quad (N_{root} \text{ x } N_{root})$	[13]
$C_5[i] = -\sum_j C_4[i,j]$	[14]
$K_{rs} = \sum_i \sum_j C_4[i,j]$	[15]
$SUF[i] = \dfrac{\sum_j C_4[i,j]}{\sum_i \sum_j C_4[i,j]}$	[16]

K_{rs} and **SUF** can be calculated directly from the compensatory matrix $\mathbf{C_4}$. In the following, we will present a reformulated form of Eq. [8] that resembles the equation that is obtained for a parallel root system. For the derivation, we refer to the appendix and we focus here on the results.

As is derived in the appendix, the matrix $\mathbf{C_4}$ in Eq. [8] can be 'factorized' in a product of two diagonal matrices: one with a diagonal that is equal to the **SUF** vector and one with a diagonal that represents a 'compensatory conductivity vector' $\mathbf{K_{comp}}$; and one matrix $\mathbf{C_7}$ which is close to the identity matrix $\mathbf{I}$:

$$\mathbf{Q} = K_{rs}\mathbf{SUF}\left(H_{eff} - H_{collar}\right) + diag\left(\mathbf{K_{comp}}\right)diag\left(\mathbf{SUF}\right)\mathbf{C_7}\left(\mathbf{H_{soil}} - \mathbf{H_{eff}}\right) \quad [17]$$

The diagonal elements of $\mathbf{C_7}$ are 1 and for each row of $\mathbf{C_7}$, the sum of the off-diagonal elements is equal to zero. To explain the meaning of K_{comp} and how it is related to K_{rs} in the parallel root system model, we consider a soil water hydraulic head distribution that is uniform except for one node i where the hydraulic head is ΔH higher than in all other nodes ($H_{soil}[j] = H_{soil}[i]$ - ΔH for all $j \neq i$). We furthermore put H_{collar} equal to H_{eff} so that there is no net uptake but only redistribution of water through the root system. Then the flow from node i to all other nodes in the root system, $\Delta Q[i]$, is:

$$\Delta Q[i] = k_{comp}[i]\Delta H \quad [18]$$

where $k_{comp}[i]$ ($L^3 T^{-1}$) represents the conductivity of the root system to transfer water from all other root elements to the root node i. From the definition of H_{eff}, it follows that:

$$H_{soil}[i] - H_{eff} = \left(1 - SUF[i]\right)\Delta H \quad [19]$$
$$H_{soil}[j] - H_{eff} = -SUF[i]\Delta H \quad for \quad all \quad j \neq i$$

Using this $\mathbf{H_{soil}}$-$\mathbf{H_{eff}}$ in Eq. [17], it follows from the soil hydraulic heads $H_{soil}[j]$ being all the same for the soil nodes j different from i and from the off-diagonal elements of a row in $\mathbf{C_7}$ summing up to zero that:

$$\Delta Q[i] = SUF[i]K_{comp}[i]\left(1 - SUF[i]\right)\Delta H \quad [20]$$

By comparing Eqs. [18] and [20], we find that $SUF[i](1-SUF[i]) K_{comp}[i] = k_{comp}[i]$.

For a root system in which all root nodes are connected in parallel to the root collar, $k_{comp}[i]$ is equal to the equivalent conductance of a serial connection of a conductance from root node i to the collar, which is $SUF[i] K_{rs}$, with a conductance from the collar to all other nodes, $(1- SUF[i]) K_{rs}$:

$$k_{comp}[i] = \left(\left(SUF[i] K_{rs} \right)^{-1} + \left(\left(1 - SUF[i]\right) K_{rs} \right)^{-1} \right)^{-1} = SUF[i]\left(1 - SUF[i]\right) K_{rs} \qquad [21]$$

This implies that for a parallel root system, $K_{comp} = K_{rs}$. It can further be shown that $\mathbf{C_7}$ is the identity matrix for a parallel root system (see appendix) so that Eq. [8] can be written as:

$$\mathbf{Q} = K_{rs}\mathbf{SUF}\left(H_{eff} - H_{collar}\right) + K_{rs}diag\left(\mathbf{SUF}\right)\left(\mathbf{H_{soil}} - \mathbf{H_{eff}}\right) \qquad [22]$$

The parallel root system is fully defined by the $\mathbf{SUF}$ and K_{rs} and the compensatory uptake is defined when the uptake distribution from a soil profile with a uniform soil water hydraulic head is known. This implies that any root system can be represented by a parallel root system with the same $\mathbf{SUF}$ and K_{rs} that simulates the same total root water uptake for any distribution of soil water hydraulic heads. However, comparing Eq. [22] with Eq. [17] shows that the compensatory uptake between the root system and its parallel root analogue differs and that $diag(\mathbf{K_{comp}})$ and $\mathbf{C_7}$ can be used as diagnostics for the difference in compensatory uptake. For the general root system, we find that $K_{comp}[i]$ is larger than K_{rs}. This means that for a certain ΔH between soil node i and all other nodes, there is more redistribution in the general root system than in the parallel root system. In the general root system, the flow from one soil-root interface to another soil-root interface does not always have to pass through the collar but can take a shorter way. A negative value of $C_7[i,j]$ means that for a given hydraulic head difference between two nodes i and j, there is more redistribution between node i and j than the average redistribution for this head difference between node i and another node than node j of the network. This means that node i is stronger than average connected to node j.

3   Upscaling:

From the matrix equations, it follows that the upscaling of the relations between the uptake rates Q and soil water hydraulic heads H_{soil} is trivial for cases when the soil water hydraulic heads are uniform in certain regions of the soil. When we assume that the soil water hydraulic heads do not change in the horizontal direction, then we can simply group and sum up all SUF values for the soil root nodes that are in the same soil horizontal soil layer and derive an upscaled $\mathbf{SUF}$ vector that describes the relative uptake from each soil layer when the soil water hydraulic heads are uniformly distributed (Couvreur et al., 2014a) (Figure 2). The upscaled matrix $\mathbf{C_4}$ that is multiplied by a vector of soil water hydraulic heads in the different soil layers is simply obtained by:

$$C_{4,upscaled}[i,j] = \sum_{k \in layer_i} \sum_{l \in layer_j} C_4[k,l] \qquad [23]$$

The dimensions of the upscaled matrices are reduced so that the number of equations that need to be solved is reduced to the number of layers in which the soil water hydraulic heads are uniform. This implies a massive reduction in the computational cost compared with the cost of solving equations for a large number of root segments that make up a 3D root architecture. Under the assumption that the soil water hydraulic heads are constant within a layer, the obtained equations are exact, independent of the soil water hydraulic heads, and need to be derived from the large set of equations for a given 3D root architecture only once. They can be used afterwards to calculate uptake from the layers for other collar and soil hydraulic heads. Based on the upscaled $\mathbf{C_4}$ and $\mathbf{SUF}$, the upscaled $\mathbf{C_7}$ and $\mathbf{K_{comp}}$ can be derived. It must be noted that $\mathbf{C_7}$ and $\mathbf{K_{comp}}$ cannot be scaled up directly by summing up elements in the $\mathbf{C_7}$ matrix and $\mathbf{K_{comp}}$ vector. When the 3D root architecture is a parallel root architecture, then the upscaled model has the same form as Eq. [22] in which the upscaled $\mathbf{SUF}$ is used. This upscaled model represents an upscaled parallel root system with each root connecting one soil layer with the to the root collar. It should

be noted that we did not derive an 'upscaled' root system topology for the exact model. In the following, we will always refer to the upscaled parallel root model. The upscaling was performed here assuming uniform soil water hydraulic heads in the horizontal direction. It can be applied for any region where soil water hydraulic heads are assumed to be uniform. The upscaled parallel root model then represents a root system with parallel roots that each connect one region with the root collar.

Figure 2: Upscaling of the SUF and C_4 matrix by simply taking the sum of elements that correspond with nodes where the soil water hydraulic heads are the same. Nodes with the same water hydraulic heads are grouped in layers and are marked with the same color. The elements of the marked blocks of the Q and SUF vectors and in the C_4 matrix are summed up.

4   Demonstrations:

In order to demonstrate the model, its upscaling, and comparison with big root and parallel root approximations, we considered in a first step an abstract 'hybrid' parallel-big root system, which is a mixture of the parallel and big root systems. It consists of three parallel branches of different length that each take up water along their length and not only at the root tip as supposed in the parallel root system. Since the water fluxes in each of the three branches are different because of their different length, the water hydraulic heads in the xylem at a given depth differ between the three roots even when the soil water hydraulic heads do not vary at a given depth. Therefore, this 'hybrid' root system represents an intermediate model that matches with neither the parallel root nor the big root model perfectly. This model should demonstrate the upscaling and the difference between the approximate models. We used a dummy parameterization of the root hydraulic properties and of the vertical distribution of the soil water hydraulic heads (i.e. the parameters were chosen to represent certain differences but the actual values of the parameters and their units were not of interest). We considered a case in which all the root segments had the same radial conductance and a case in which the radial conductance at the root tips were a factor 10 larger.

In a second step, we considered a single root with either constant or changing root hydraulic parameters along the root axis.

In a third step, we considered root systems that correspond in terms of complexity and parameterization to more realistic root systems and represent three different crops: grass, maize and sunflower.

4.1 Simple hybrid root system:

a) Hybrid parallel-big root system

$$\mathbf{Q} = K_{rs}\left(H_{eff} - H_{collar}\right)\mathbf{SUF} + diag\left(\mathbf{SUF}\right)diag\left(\mathbf{K_{comp}}\right)\mathbf{C_7}\left(\mathbf{H_{soil}} - \mathbf{H_{eff}}\right)$$

b) Big root

$$\mathbf{Q} = K_{rs,br}\left(H_{eff,br} - H_{collar}\right)\mathbf{SUF}_{br} + diag\left(\mathbf{SUF}_{br}\right)diag\left(\mathbf{K_{comp,br}}\right)\mathbf{C_{7,br}}\left(\mathbf{H_{soil}} - \mathbf{H_{eff,br}}\right)$$

c) Parallel root with bottom-up parameterization

$$\mathbf{Q} = K_{rs}\left(H_{eff} - H_{collar}\right)\mathbf{SUF} + K_{rs}diag\left(\mathbf{SUF}\right)\left(\mathbf{H_{soil}} - \mathbf{H_{eff}}\right)$$

d) Parallel root with top-down parameterization

$$\mathbf{Q} = K_{rs}\left(H_{eff,Kx,\inf} - H_{collar}\right)\mathbf{SUF}_{Kx,\inf} + K_{rs}diag\left(\mathbf{SUF}_{Kx,\inf}\right)\left(\mathbf{H_{soil}} - \mathbf{H_{eff,Kx,\inf}}\right)$$

Figure 3: Resistance nets representing the hybrid parallel-big root system consisting of three primary root branches of different length a); and approximations by: the big root model b); the parallel root model using a bottom-up parameterization c); and the parallel root model with a top-down parameterization d). The closed circles represent root nodes and the open circles soil nodes; the brown and green resistors represent radial and axial root segment conductances, respectively. The approximate models describe upscaled root water uptake from 4 depths. The SUF$_{br}$, K$_{rs,br}$, K$_{comp,br}$ and C$_{7,br}$ of the big root model are calculated from the segment axial and radial conductances that are arranged following the big root topology in parallel within a soil layer from which upscaled big root segment conductances K$_{r,up,br}$ and K$_{x,up,br}$ are calculated (top-down parameterization). The SUF and K$_{rs}$ of the parallel root model with bottom-up parameterization c) are matched to those of the upscaled hybrid model by adapting the axial conductance K$_{x,up,eff}$ of the segment that connects the xylem node at a certain depth to the collar node. The SUF of the parallel root model with top-down parameterization assuming infinite K$_{x,up}$ d) is derived from the distribution of radial root segment conductances with depth, which are scaled to K$_{r,up,eff}$ so that K$_{rs}$ matches that of the hybrid root system. The equations below the resistance nets represent the equations that calculate the upscaled water uptake Q in a horizontal layer.

Figure 3 a) shows the hybrid parallel-big root system that consists of three primary root branches of different length which take up water from up to 4 different depths. This root system was scaled up to a model that describes uptake from the 4 depths assuming that the soil water hydraulic head is uniform at a given depth (the exact model). The upscaled **SUF**, which represents the uptake by all root segments at a certain depth, was equal to the sum of the SUFs of the individual root segments at that depth. The upscaled hybrid parallel-big root system model was approximated by parallel and big root system models. The big

root approximation assumes that the root segments are organized and connected following the a-priori defined big root architecture so that the upscaled axial $K_{x,up,br}$ and radial $K_{r,up,br}$ conductance in a certain layer is the sum of the axial and radial conductances of the individual root segments in that layer (Figure 3 b). Since we assume a-priori a certain topology of the root segments and parameterize the model directly based on the number of root segments in a soil layer and their properties (radial and axial conductances), we called this a top-down parameterization. For the parallel root approximation, we considered a root system with the same **SUF** and K_{rs} as the upscaled hybrid model (Figure 3 c). For a given distribution of radial conductances, K_{rs} and **SUF** can be defined by adapting an upscaled effective $K_{x,up,eff}$ of virtual root branches that connect a certain depth with the root collar. This parameterization, which is based on calculations for the 3D hydraulic root architecture, corresponds with a bottom-up parameterization. For the upscaled parallel root model, the number of parameters that needs to be defined is equal to the number of soil layers, ndepths: ndepths $K_{x,up,eff}$ values or K_{rs} and ndepths-1 SUF values (sum of SUF =1). In contrast, the big root model requires 2 ndepths parameters. Unlike for the parallel root system, there is no simple relation between K_{rs} and **SUF** on the one hand and the compensatory uptake term on the other for the big root model. Therefore, the structure of the big root model does not lend itself to calculating its parameters directly from characteristics of the 3D hydraulic root architecture in a bottom-up approach. The third model that we considered is a parallel root model with an infinitely large axial conductance ($K_{x,up} = \infty$) in which the **SUF** is derived in a top-down approach directly from the distribution of the upscaled radial conductances, $K_{r,up,eff}$, with depth. The K_{rs} of this root system was adjusted to the K_{rs} of the hybrid root system, which comes down to a scaling of the radial conductance of all root nodes with the same factor.

We considered two parameterizations of the root hydraulic conductances. In the first case, the conductances of all root segments are uniform: K_x=10 and K_r =1. In the second case, the radial root hydraulic conductance is larger at the root tips (K_r=1) than in the other parts along the primary roots (K_r=0.1). To evaluate the effect of a non-uniform hydraulic head in the soil, the soil water hydraulic heads varied from top to bottom as: -0.5, 0, 0.5, 1 and were assumed to be the same for root nodes at the same depth. The hydraulic head at the root collar was set to -1. The K_{rs}, **SUF** and K_{comp} and their upscaled values for the hybrid root system and the three approximations are given in Table 2 and Table 3 for the root system with homogeneous root segment conductances and for the root system with higher radial conductances at the root tips, respectively. The root water uptake profiles that are simulated by the different models for the two parameterizations of the root segment conductivities are given in Figure 4 and Figure 5.

The parallel root system with a top-down parameterization and using the distribution of root segment radial conductances with depth to estimate **SUF** overestimates the **SUF** deeper in the soil profile and underestimates it at shallower depths. The resistance to axial flow reduces the SUF of distal root segments compared to the SUF of more proximal root segments. The big root model can better account for the impact of the axial resistance on the **SUF**. However, the assumption of equal xylem hydraulic head in all root segments at a certain depth leads to an underestimation of the SUF of the proximal root segments (Table 2) . This underestimation was not important when the radial conductance was larger near the root tips (Table 3).

For a non-uniform distribution of the soil water hydraulic head, which increased with depth, the uptake at greater depths increased and that at shallower depths decreased as compared to the uptake under uniform soil water hydraulic head (Figure 4 and Figure 5). All models reproduced this compensation of root water uptake. The parallel root model with bottom-up parameterization, which used the exact root system **SUF** and K_{rs}, underestimates the root water uptake compensation whereas the big root model overestimates it. The parallel root model uses K_{rs} to calculate the compensatory uptake and K_{rs} was smaller than K_{comp} (Table 2 and Table 3). The big root model overestimates the compensation since it assumes that all root segments in a certain layer are directly connected to all the root segments in the overlying or underlying layers and that the xylem hydraulic heads are the same in all root segments at a certain depth. This implies that redistribution of water between the soil layers via the root system can occur directly without flow having to pass the collar first before it returns to another layer. The K_{comp} that is derived for the big root model is only slightly higher, except for the deepest root node, than the K_{comp} of the exact model. The larger uptake from the deeper layer simulated by the big root model is therefore linked to the larger SUF in the

deeper soil layers. This is also the case for the parallel root model with bottom-up parameterization for which the higher *SUF* at greater depths in combination with higher soil water hydraulic heads at greater depths led to a larger simulated water uptake.

Also of interest is that the upscaled K_{comp} values are not equal to the average of the K_{comp} values of the root nodes in a soil layer. For the top layer, the upscaled K_{comp} is even larger than the largest K_{comp} value of the three primary root branches. Smaller radial conductance away from the root tips led to a root system that behaves more like a parallel root system (Figure 5). This is reflected in the K_{comp} values that are closer to K_{rs} and the $\mathbf{C_7}$ matrix that is closer to the identity matrix than the $\mathbf{C_7}$ matrix of the hybrid parallel-big root system with uniform root segment hydraulic properties (Table 3). The higher radial root segment conductances near the root tips make that water transfer between two soil layers through root tips in these soil layers, which passes via the root collar, is more efficient than water transfer between a root tip segment and a root segment with lower radial conductance that is directly connected to it. In the big root model, the root tip segment with higher radial conductance in one layer is assumed to be directly linked to the root tip segment in another layer so that the water flow between these layers occurs more efficiently than via the root collar. This is reflected in the higher K_{comp} and the larger deviation of the $\mathbf{C_7}$ matrix from the identity matrix for the big root model than for the hybrid parallel-big root model, which leads to an overestimation of the root water uptake compensation by the big root model.
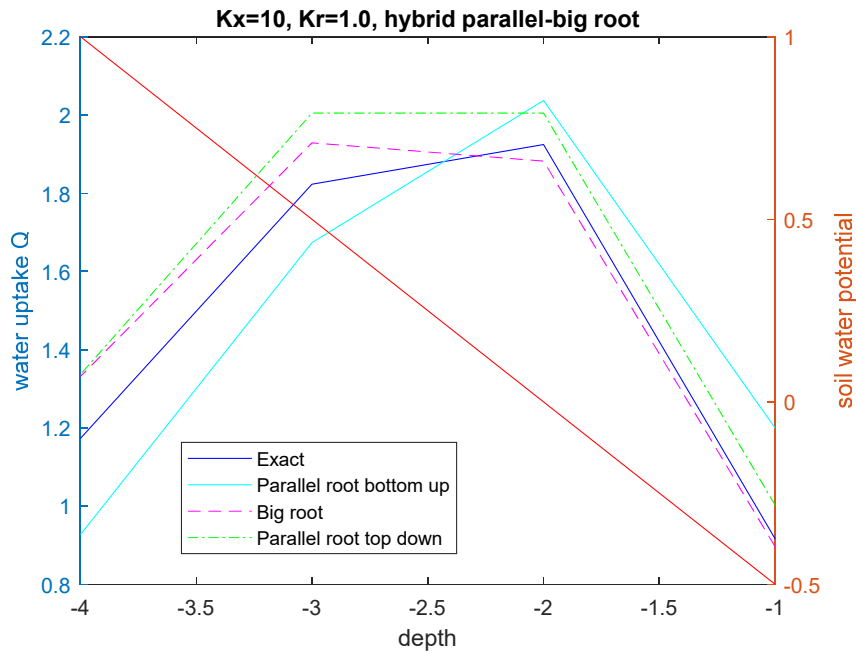
Figure 4: Upscaled water uptake profile (left axis) and soil water potential distribution (right axis, red line) for the hybrid parallel-big root system with constant radial conductances along the primary root branches; the parallel root model with bottom-up parameterization (SUF and K$_{rs}$ derived from exact model); the big root model; and the parallel root model with top-down parameterization.
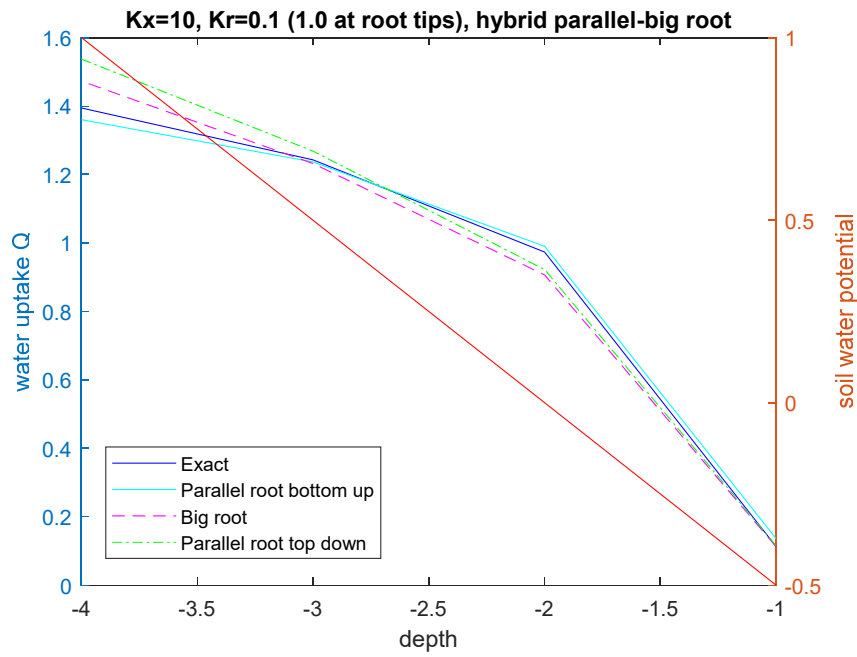
375 **Figure 5: Upscaled water uptake profiles (left axis) and soil water potential distribution (right axis, red line) for the hybrid parallel-big root system with radial conductances along the primary root branches that vary along the branches (radial conductance is 1 at root tips and 0.1 at other nodes); the parallel root model with bottom-up parameterization (SUF and K_{rs} derived from exact model); the big root model; and the parallel root model with top-down parameterization.**

Table 2: K_{rs}, SUF, K_{comp} and upscaled values and C_7 matrices for the hybrid parallel-big root system with constant K_r along the roots , the big root system and the parallel root system (with infinite K_x) using top-down parameterization

	Hybrid Parallel-Big root				Big root (top-down)	Parallel (top-down)
	$K_r=1$, $K_x=10$, $K_{rs}= 6.0147$				$K_{rs}= 6.1122$	Inf K_x, $K_{rs}= 6.0147$
	Prim. root 1	Prim. root 2	Prim. Root 3	Upscaled		
Depth	SUF	SUF	SUF	SUF	SUF	SUF
1	0.1396	0.1319	0.1273	0.3988	0.3908	0.3333
2	0.1269	0.1108	0.1010	0.3387	0.3299	0.3333
3		0.1007	0.0848	0.1855	0.1920	0.2222
4			0.0771	0.0771	0.0873	0.1111
	K_{comp}	K_{comp}	K_{comp}	K_{comp}		
1	6.65	7.13	7.44	7.52	7.68	
2	6.70	7.98	8.94	8.41	8.65	
3		8.09	10.09	9.35	9.39	
4			10.26	10.26	10.00	

C_7 matrix of the upscaled hybrid parallel-big root system

1	0	0	0
0.042	1	-0.030	-0.012
0.078	-0.014	1	-0.064
0.106	0.017	-0.123	1

C_7 matrix big root system

1	0	0	0
0.044	1	-0.030	-0.014
0.071	-0.022	1	-0.050
0.091	0	-0.091	1

Table 3: K_{rs}, SUF, K_{comp} and upscaled values and C_7 matrices for the hybrid parallel-big root system with variable root radial root segment conductances along the roots (K_r=0.1 along roots except at root tip K_r=1), for the big root system, and for the parallel root system (with infinite K_x) using top-down parameterization

	Hybrid Parallel-Big root					Big root (top-down)	Parallel (top-down)
	K_r=1, K_x=0.1, K_{rs}= 2.7673					K_{rs}= 2.7673	Inf K_x, K_{rs}= 2.7673
	Prim. root 1	Prim. root 2	Prim. root 3	Upscaled			
Depth	SUF	SUF	SUF	SUF		SUF	SUF
-1	0.0328	0.0328	0.0328	0.0984		0.0984	0.0833
-2	0.2984	0.0298	0.0298	0.3580		0.3576	0.3333
-3		0.2709	0.0270	0.2979		0.2979	0.3056
-4			0.2457	0.2457		0.2462	0.2778
	K_{comp}	K_{comp}	K_{comp}	K_{comp}			
-1	3.0274	3.0295	3.0313	3.0485		3.0485	
-2	2.8067	3.3170	3.3213	2.9419		3.3373	
-3		2.8815	3.6389	2.9847		3.5590	
-4			2.9892	2.9892		3.5898	

C_7 matrix of the upscaled hybrid parallel big-root sytem

1	0	0	0
-0.004	1	0.002	0.002
-0.002	0.007	1	-0.005
-0.002	0.008	-0.006	1

C_7 matrix of the big root system

1	0	0	0
0.009	1	-0.005	-0.004
0.014	0.017	1	-0.031
0.015	0.02	-0.035	1

4.2 Single root branches

We considered two single root branches, one with homogeneous (intrinsic) root segment conductances (k_x= 0.171 cm³ d^{-1}, k_r= 1.81 10^{-4} d^{-1}) and one with conductances that changed along the root axis due to maturation of the root tissue (Figure 6). This generally leads to an increase in axial conductance and a decrease in radial conductance with age or distance from the root tip (Doussan et al., 1998;Doussan et al., 2006;Zarebanadkouki et al., 2016;Couvreur et al., 2018;Meunier et al., 2018b). The "reference " exact model was a 50 cm long root discretized in 0.5 cm long root segments.

The collar water hydraulic head was assumed to be -4000 cm and the soil water hydraulic head varied linearly between -3000 cm at the soil surface and 0 cm at the lowest depth of the root system. The upscaled model considered 2 cm long segments.

As expected, the big root system matches nearly perfectly with the exact model (Figure 7). The deviations are due to the upscaling and the variations of soil water and xylem hydraulic heads along a root segment that is represented by a single node (Bouda, 2019). Nevertheless, the close agreement indicates that the 0.5 cm discretization of the root approximates the exact solution of the flow equation in the single root well. Details on the convergence of this discretization and on exact solutions for arbitrary root segment sizes (given that the soil water potentials do not vary along the root segments) are given by Meunier

et al. (2017b);Meunier et al. (2017c). For large root segment sizes or small K_x, when the discrete approximation becomes inaccurate, exact solutions can be implemented in a complex root architecture (see Bouda (2019)) but this should lead to a different coefficient matrix $\mathbf{C_4}$ and $\mathbf{C_5}$ vector. The parallel root model with a top-down parameterization that derives the *SUF* based on the radial root segment conductances assuming an infinite K_x overestimates the *SUF* in the distal part of the root since the impact of the axial resistance to flow is not considered. For a larger soil water hydraulic head near the distal end of the root, the overestimation of the *SUF* in this region results in an overestimation of the root water uptake from the deeper soil and an overestimation of the apparent root water uptake compensation. The opposite is the case for the parallel root system with a bottom-up parameterization, which uses the exact $\mathbf{SUF}$. This model underestimates the uptake near the distal end of the root due to an underestimation of K_{comp} by the parallel root model. However, for a root with non-uniform root segment conductances, uptake simulated with this parallel root system represents nearly perfectly the exact uptake and even slightly better than the big root system. Even for a single root, which can be considered to be a 'perfect' big root system, the parallel root model may perform quite well when it uses the exact $\mathbf{SUF}$. This is even better when root segment conductivities vary along the root. The K_{comp} profiles and $\mathbf{C_7}$ matrices, which are shown for the two root systems in Figure 8, may be used as diagnostics of the approximation of the root water uptake by the parallel root model. Rather than the absolute values of the ratios of K_{comp}/K_{rs} and of the entries in the $\mathbf{C_7}$ matrix, the distributions of these values along the root profile seem to indicate whether a parallel root model can describe the uptake profile. For the root with uniform root segment conductances, larger values of K_{comp}/K_{rs} and off-diagonal entries in $\mathbf{C_7}$ that deviated from zero were distributed more over the entire root length whereas for the root with non-uniform root segment conductivities, these larger values and deviations where concentrated near the root tips.

425
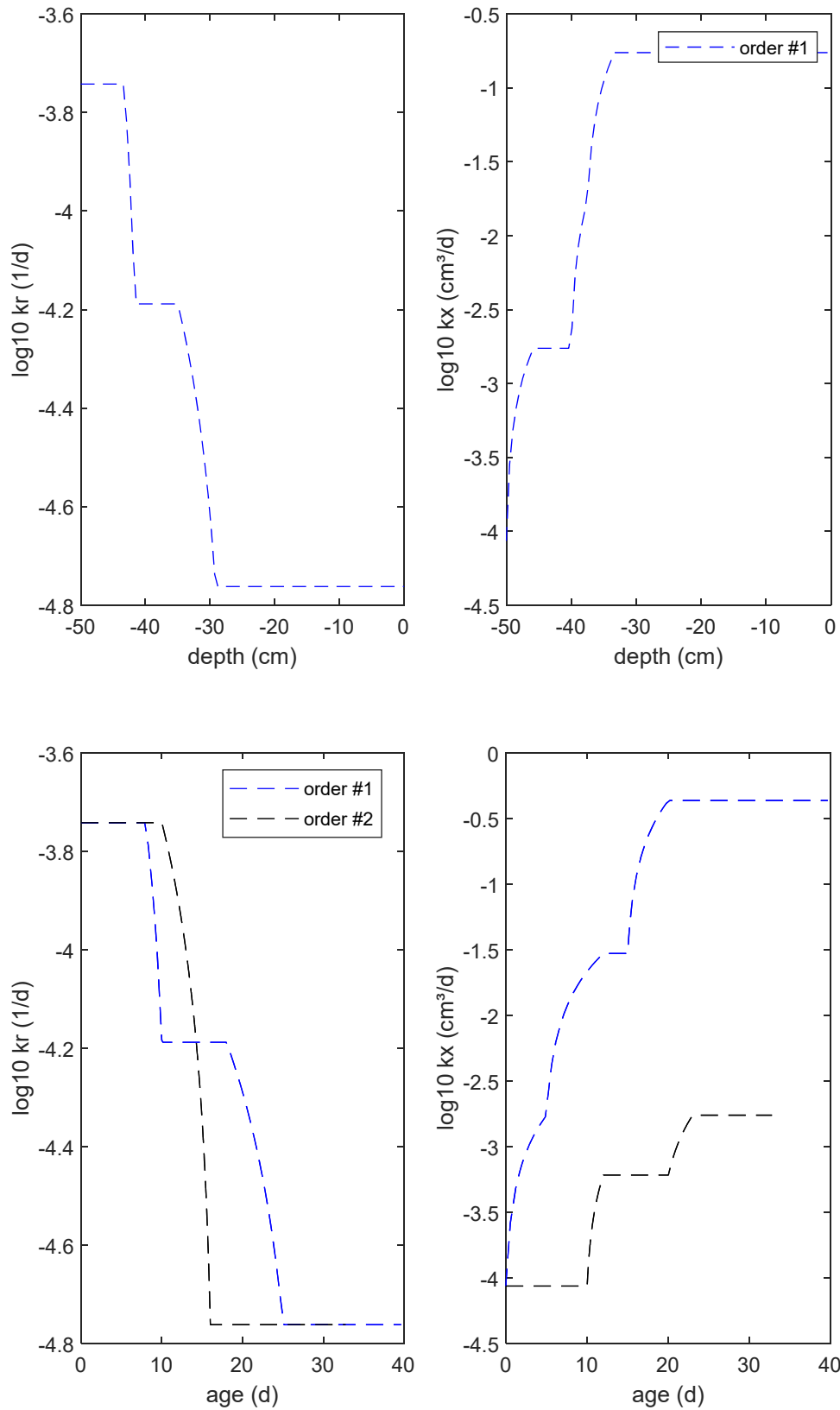
Figure 6: Radial (left), k_r, and axial (right), k_x, intrinsic root conductances for the single root (top) and root system architectures (bottom). For the single root, conductances are plotted versus depth and for the root system architectures versus root segment age.

a)   b)
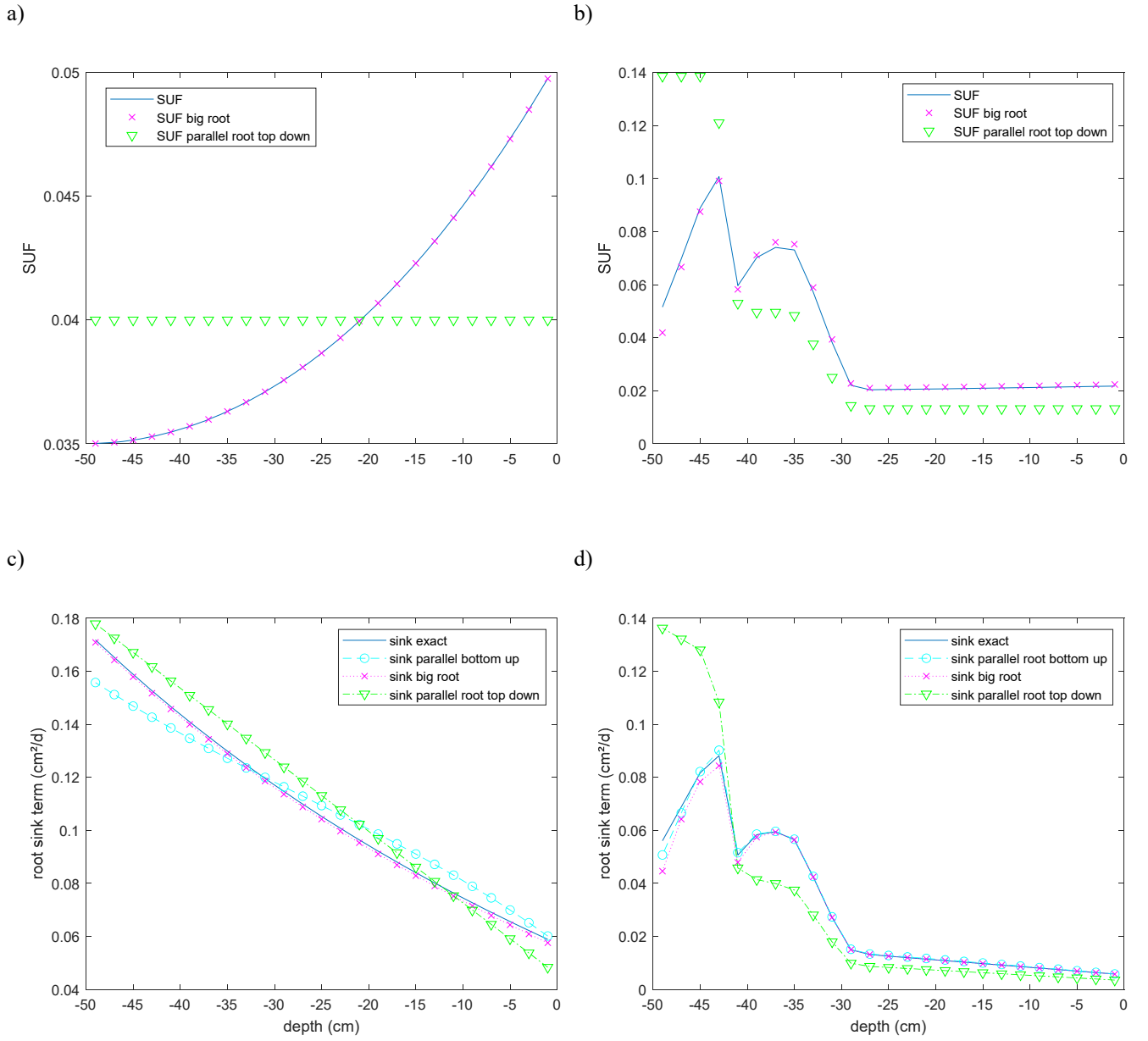
Figure 7: **Standard uptake for homogeneous soil water potential (SUF) (a,b) and root sink term for a linear increase of water**
potential with depth (c,d) of a single root branch with uniform (a,c) and age dependent (b,d) root segment conductances.
Approximations are calculated for the parallel root with a bottom-up parameterization using the exact SUF and K_{rs}, the big root
model, and parallel root model with a top-down parameterization with SUF estimated from the radial root segment conductivities.
Sink terms are divided by the thickness of the soil layer, 2cm, over which the root segment sink terms are summed.

430

a)   b)
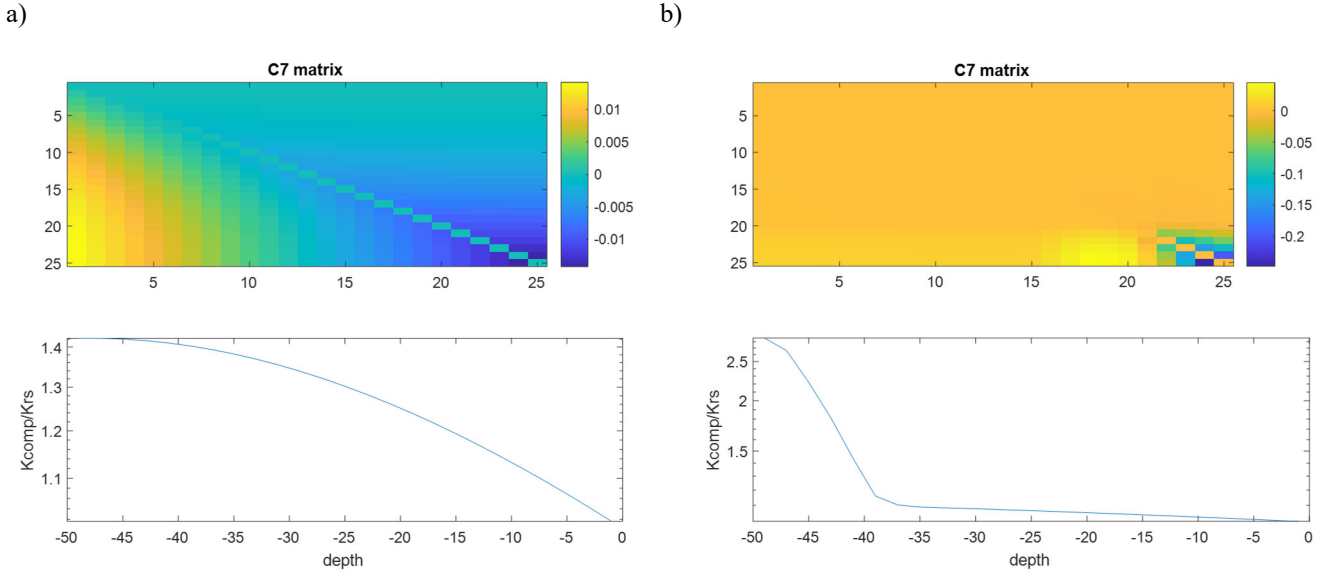
Figure 8: C_7 matrices and profiles of the ratio of K_{comp}/K_{rs} of the exact single root model with uniform (a) and non uniform (b) root segment hydraulic conductances along the root. The labels on the axes of the C_7 matrices represent the root segment numbers, which increase from the proximal to the distal end of the root, i.e. from top to bottom. For visualization, the diagonal elements of the C_7 matrix were set to 0.

4.3   Realistic root systems:

We generated root systems of three different plants: maize, sunflower and grass using the CRootBox shiny app (https://plantmodelling.shinyapps.io/shinyRootBox/) (Schnepf et al., 2018). The grass root system with several primary roots and few laterals may represent a parallel root system. The maize root system with several primary roots that each take up water along their axis by lateral roots may represent a hybrid parallel big root system whereas the sunflower root system with a single main root and several lateral roots might rather represent a big root system (Figure 9). The intrinsic radial and axial root segment conductances depended on the root order and varied with age (Figure 6). We assumed that this relation between root age and segment conductance did not vary between the crops. It should be noted that the root architectures and intrinsic root segment conductances were chosen to illustrate the difference between the different root water uptake modeling approaches for more realistic root systems. However, the derived root system characteristics should not be interpreted as the characteristics of a certain crop. As for single root branch simulations, the collar water potential was -4000 cm, the soil water potential at the soil surface -3000 cm and 0 cm at the maximal rooting depth of the root system. The **SUF** and root water uptake distributions were scaled up to and derived for 2cm thick horizontal soil layers yielding 1D vertical profiles.

For the parameterization of the big root model, we calculated the axial conductance of the big root for each soil layer i, $K_{x,up,br}[i]$, from the length, orientation, and intrinsic axial conductances of all the root segments in that layer as follows. First we calculated an 'effective' intrinsic axial conductance for flow in the vertical direction in the ith soil layer, $k_{x,eff}[i]$

$$k_{x,eff}[i] = \frac{\sum_j l[j] |\cos(\alpha[j])| k_x[j]}{\sum_j l[j]} \qquad [24]$$

where $\alpha[j]$ the angle of the segment with the vertical and j the indices of root segments in layer i. To obtain $K_{x,up,br}[i]$ we multiplied the effective intrinsic axial conductance by the number of roots that cross the layer and divided it by the layer thickness. The number of roots that cross the layer i is calculated from the sum of the vertical increments of the root segments divided by the layer thickness so that we obtained:

$$K_{x,up,br}[i] = \frac{k_{x,eff}[i]\sum_j l[j]\left|\cos(\alpha[j])\right|}{\Delta z[i]^2} \qquad [25]$$

The radial conductance of the big root system in layer i, $K_{r,up,br}[i]$ was calculated by simply adding up the radial conductances of the root segments.

For the parallel root system with bottom-up parameterization, we used the **SUF** and K_{rs} values of the exact upscaled model. For the parallel root model with the top-down parameterization, assuming an infinite K_x, the **SUF** was directly calculated from the distribution of the radial root segment conductances that were upscaled as in the big root model:

$$SUF[i] = \frac{K_{r,up,br}[i]}{\sum_i K_{r,up,br}[i]} \qquad [26]$$

To account for the effect of resistance to axial flow, the exact K_{rs} is used in the top-down parameterized parallel root model. It should be noted that Eqs. [24], [25], and [26] use information about root segments such as their orientation, age and root type dependent conductance, and surface which is mostly not used or available to parameterize macroscopic hydraulic root water uptake models. Mostly, the root segment conductances and root radii are assumed to be constant so that root length density is used to estimate the hydraulic properties. Since we focus in this paper on the differences between different model structures, we used the more detailed information to avoid differences due to differences in information that was used for parameterization. The root system conductances that are estimated from the root segment conductances considering the 3D hydraulic root architectures, K_{rs}, or using a big root representation, $K_{rs,br}$, are given in Table 4. The root system conductances for sunflower are considerably smaller than those of maize and grass. This is attributed to sunflower having only one single tap (primary) root with a high intrinsic axial conductance (Figure 6) versus maize and grass having many primary roots. $K_{rs,br}$ is larger than the exact K_{rs}. The top-down parameterization of the big root model (Eqs. [24] [25]) in combination with the assumption that the root architecture can be represented by a single big root leads to an overestimation of the root system conductance. This was also observed for the simple hybrid big-parallel root model (Table 2).

For the grass root system, which consists of several short primary roots with high axial conductance, **SUF** is almost not sensitive to the assumed root architecture (Figure 10 e). For the maize and sunflower root systems, the parallel root system using a top-down parameterization and assuming no axial resistance to flow underestimated the *SUF* at shallower depths and overestimated it at intermediate (maize) and deeper (sunflower and maize) depths (Figure 10 a,c). Not considering axial resistance to flow leads to an overestimation of the uptake capacity of the distal ends of roots, especially when the axial conductivity decreases and the radial conductance increases towards the root tip (see also Figure 7 b). Depths where the *SUF* is strongly overestimated correspond with depths with high densities of younger lateral roots. The **SUF** of the big root model corresponded better with the exact **SUF**. But, in the big root model, the axial resistance to flow from the distal ends of the deep primary roots to the collar is apparently overestimated and the *SUF* in the deeper soil layer underestimated. In the big root model, the xylem water potentials in the secondary and primary roots in a certain layer are assumed to be equal since it is assumed that all root segments in a layer act in parallel. However, because of the lower axial conductance of secondary roots (see Figure 6) which are connected in series to primary roots, the xylem water heads can be considerably higher in the secondary than in the primary roots in a certain layer. Assuming similar xylem water heads in secondary and primary roots in a certain soil layer reduces the xylem heads in the secondary roots and generates too much uptake by the secondary roots in that layer. An overestimation of uptake in a more 'downstream' or shallower soil layer will lead to an underestimation in the more 'upstream' or deeper layers. These effects may explain the underestimation of the *SUF* below approximately 50 cm depth in the maize and sunflower root systems that is compensated by an overestimation in shallower depths.

The non-uniform soil water hydraulic heads resulted in an increased uptake deeper in the soil profile (compare the shape of the **SUF** and sink term profiles in Figure 10). For the grass root system, the sink distributions for the different models are very

similar. The higher uptake predicted by the big root model is due to the higher $K_{rs,br}$ than the true K_{rs}. For the other root system models, the differences between the sink term distributions of the exact model, the big root model, and the parallel root model with top-down parameterization assuming infinite axial conductance are caused by differences in K_{rs}, **SUF**, and compensatory uptake resulting from approximations of K_{comp} and the **C7** matrix (Figure 11). The parallel root model with bottom-up parameterization that uses the exact K_{rs} and **SUF** profile but approximates K_{comp} by K_{rs} and **C7** by the identity matrix, predicts almost the same sink term distribution profile as the exact model. This bottom-up parallel root model slightly underestimates the compensatory root water uptake, i.e. too much uptake near the soil surface and too little deeper in the soil profile. The exact K_{comp}/K_{rs} trace and **C7** matrix of the root systems (Figure 11) suggest the largest deviations between the sink term distributions of the exact model and the bottom-up parallel root model for the sunflower root system, which corresponds with the results shown in Figure 10. The impact of approximations of K_{comp} and the **C7** matrix on the sink term distribution is apparently of second order importance compared to the impact of the estimated K_{rs} (big root model) and **SUF** (big root model and top-down parallel root model with infinite axial conductance).

Table 4: Root system conductances, K_{rs} and root system conductances of the big root model, $K_{rs,br}$ estimated from root segment conductances,

	K_{rs} (cm²/d)	$K_{rs,br}$ (cm²/d)
Maize	0.0576	0.0781
Sun flower	0.00555	0.0068
Grass	0.045	0.0489

a)
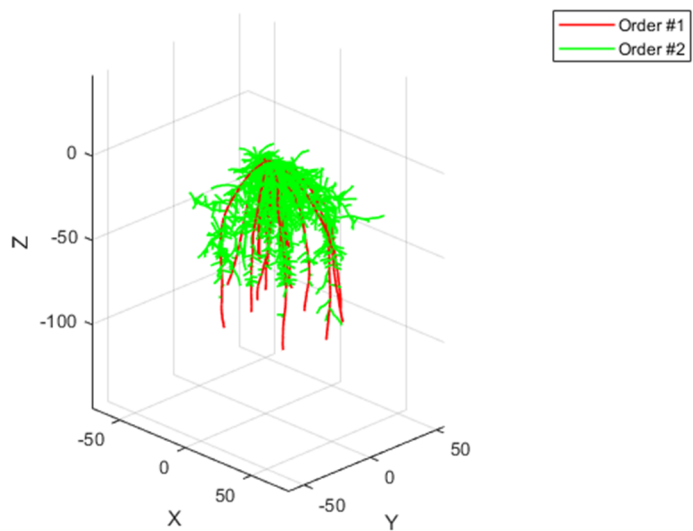
b)
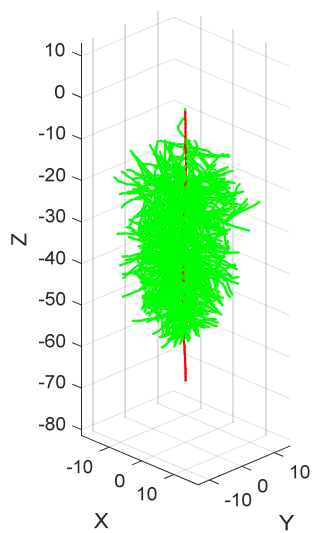
c)
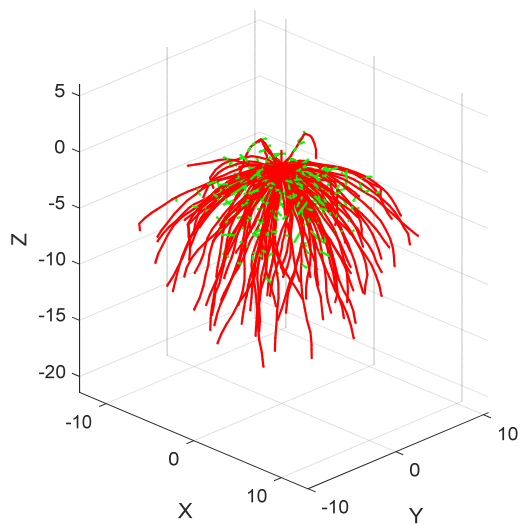
Figure 9: Root systems generated with the CRootbox shiny app: a) maize, b) sunflower, c) grass. Colors refer to the root order.
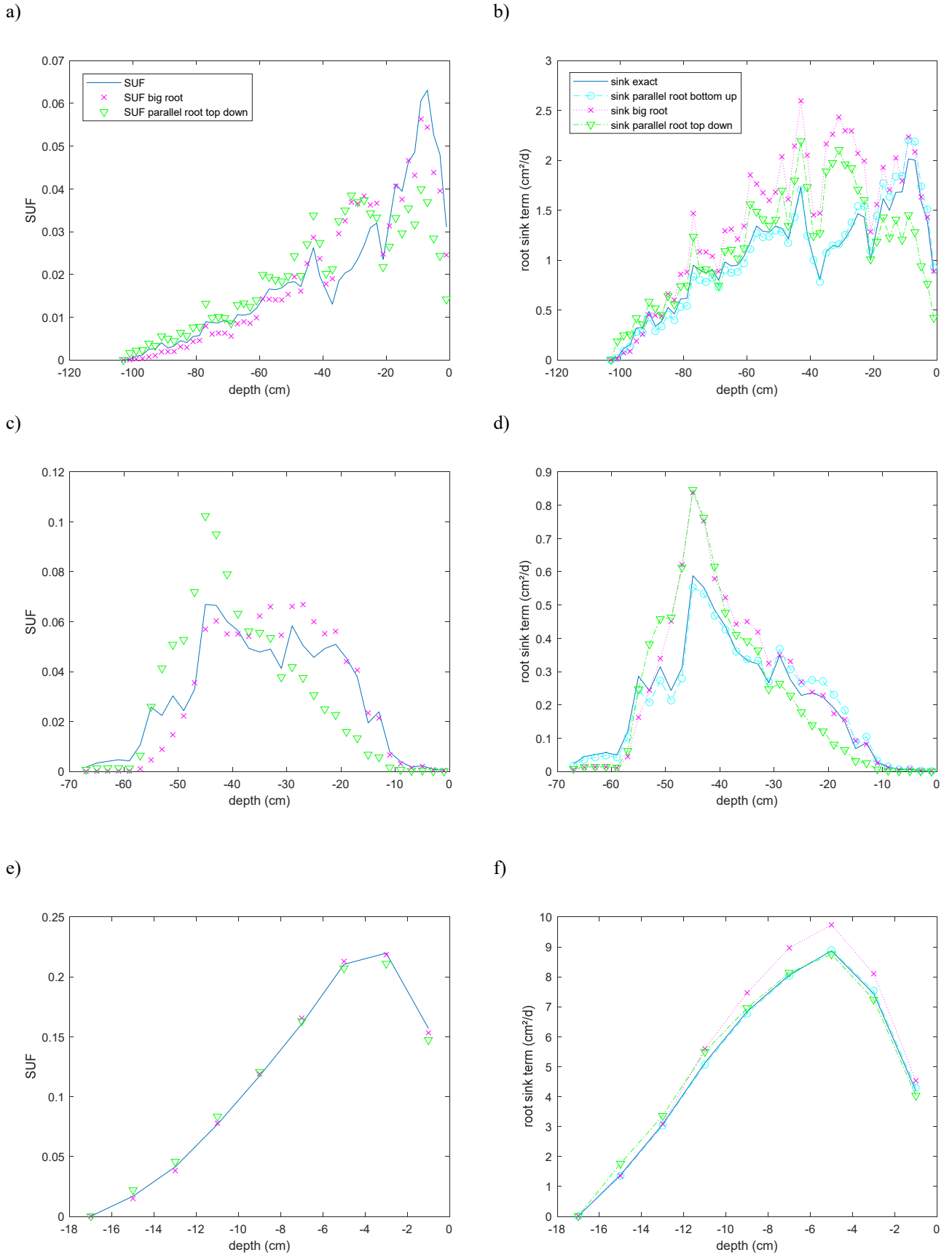
Figure 10: Depth profiles of scaled up Standardized Uptake Fractions (SUF) (a,c,e) and sink term distribution normalized by the considered soil layer thickness (2 cm) for a non-uniform soil water potential distribution (-3000 cm at the soil surface and 0 cm at the maximal root depth) (b,d, f) for maize (a,b), sunflower (c,d) and grass (e,f) root systems shown in Figure 9. Approximations are calculated for the parallel root with a bottom-up parameterization using the exact SUF and K_{rs}, the big root model, and parallel root model with a top-down parameterization with SUF estimated from the radial root segment conductivities. Sink terms are divided by the thickness of the soil layer, 2cm, over which the root segment sink terms are summed.

515

a)
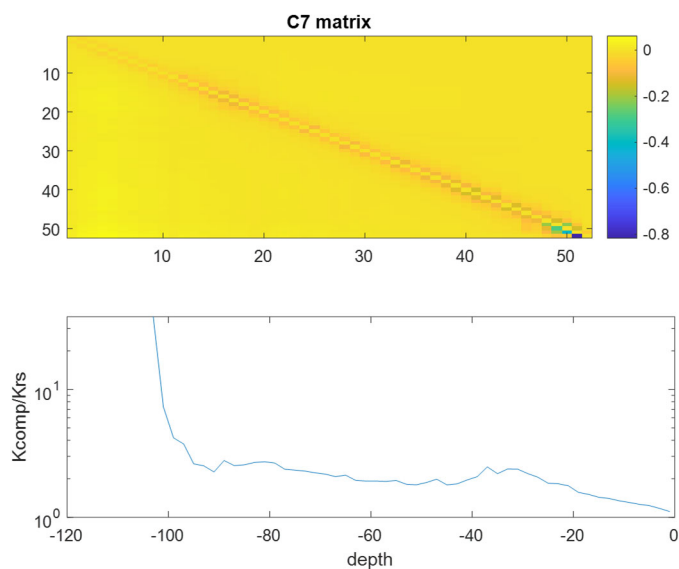
b)
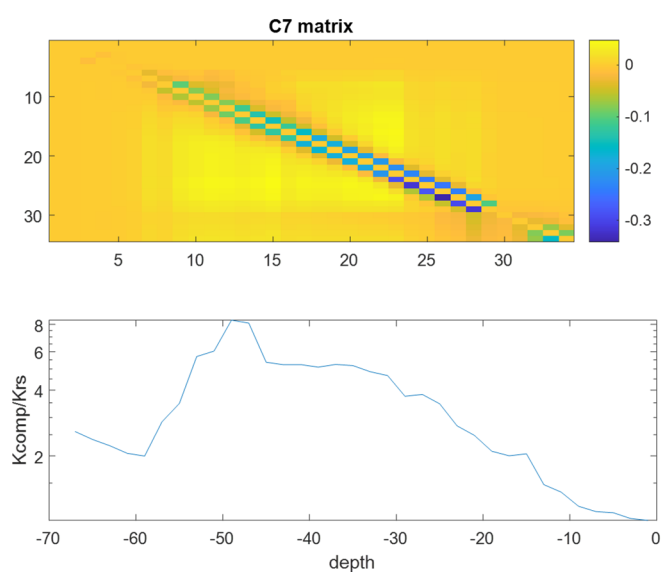
c)
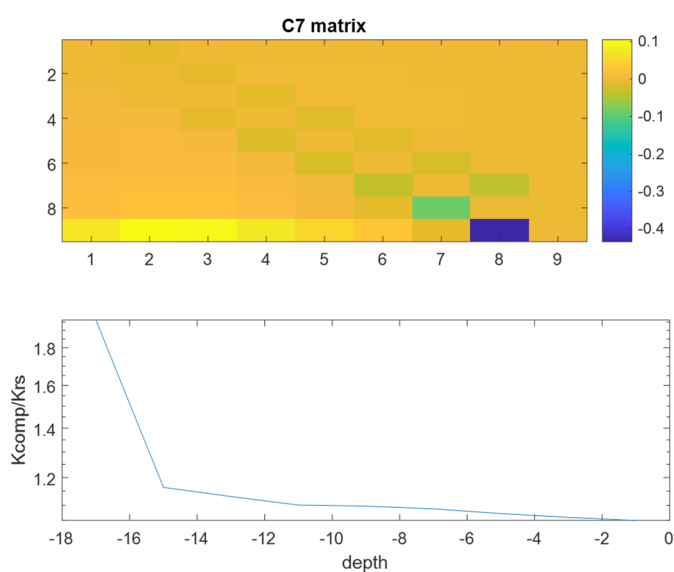
520   **Figure 11: C₇ matrices and ratios of Kcomp/Krs of the exact model for the maize a), sunflower b), and grass c) root systems**

5   Discussion and Conclusion

We analysed the equation that describes water flow in a network of root segments, which constitutes a root system architecture (RSA) and reformulated it into a form that lends itself to upscaling and to deriving simpler or parsimonious root water uptake models.

In line with Couvreur et al. (2012), we deduced that the total uptake by a root system is a simple function of a weighted soil water hydraulic head and the weights are equal to the water uptake by the RSA in a uniform soil water hydraulic head field. The root system conductance, K_{rs}, and the uptake distribution for uniform soil water hydraulic head, i.e. the standardized uptake fraction **SUF**, are the two properties of the root system that define the relation between the transpiration, the collar hydraulic head, and the distribution of the soil water potentials. This implies that for any distribution of soil water hydraulic heads that leads to the same weighted hydraulic head, transpiration rate and collar hydraulic head are uniquely related.

We found that the uptake distribution is the sum of the uptake for the case of a uniform soil water hydraulic head, i.e. the weighted hydraulic head, and a correction or compensation term that depends on the difference between the local and weighted soil water hydraulic head. Unlike how it is defined in other approaches (Simunek and Hopmans, 2009;Jarvis, 2011), this compensation term does not depend on the collar hydraulic head or transpiration rate, which is a consequence of the compensation being a passive redistribution process that is not influenced by the transpiration rate as long as the soil water hydraulic heads do not change by the plant water uptake.

When soil water hydraulic heads are assumed to be uniform in certain regions, e.g. in horizontal soil layers, the upscaling of the root water uptake model is trivial and leads to the same form as the detailed model. Whether soil water hydraulic heads remain uniform during root water uptake depends on spatial distribution of the root segments and on the water redistribution in the soil that cancels out spatial variations in root water uptake (Couvreur et al., 2014a). Further work is needed to evaluate this assumption and to develop upscaling methods when soil water hydraulic heads cannot be assumed to be uniform in the horizontal direction.

The simplified root architectures that are used in land surface models (LSM), big root and parallel root models, are special cases of RSAs and the root water uptake models for these architectures can be cast in the same form as the model for a general RSA. For the parallel root model, we could show that the root water uptake model is fully defined by the K_{rs} and **SUF** of the root system. K_{rs} and **SUF** of the parallel root system model that is used in a 1D LSM assuming horizontally uniform soil water hydraulic heads can be derived directly and exactly from upscaled K_{rs} and **SUF** of a general root system. The impact of the root segment connections and their root hydraulic properties are directly represented in the K_{rs} and **SUF**, which can be calculated and scaled up without making any simplifying assumptions about the RSA. The bottom-up approach to parameterize a parallel root model from 3D RSA models is therefore straightforward. For the big root model, we could not find such a simple relationship and upscaling was carried out by first deriving the effective conductances of the big root segments based on the intrinsic conductances of the root segments in a certain layer. From the obtained big root model conductances, K_{rs} and **SUF** were derived. Since the derivation of big root conductances cannot account exactly for the 3D RSA and its hydraulic properties, the obtained K_{rs} and **SUF** for the big root model are approximations. Another approach that could be pursued is to derive upscaled K_{rs} and **SUF** directly from the 3D RSA (as was done for the parallel root model) and fit the conductances of the big root model. However, for each layer, only one SUF value is available whereas two conductances (radial and axial) need to be estimated for the big root segment in that layer. This implies that more information about water uptake by the 3D RSA is required, such as compensatory uptake, in order to parameterize the big root model conductances. The big root model lends itself less for a bottom-up parameterization approach than the parallel root model. K_{rs} and **SUF** of the parallel root model could also be estimated following a top-down approach from intrinsic root segment conductances without solving the 3D RSA model. But, then it needs to be assumed that the axial root segment conductances are large so that they do not limit the uptake. This

assumption led, for the considered root segment hydraulic properties, to an overestimation of the uptake by the distal parts of the roots.

When the exact K_{rs} and **SUF** are used in the parallel root system model, the approximations in the parallel root system model lead to an underestimation of redistribution of the water uptake for non-uniform distributions of the soil water hydraulic head. However, the typical distribution of radial conductances along a root with lower radial conductances in older more proximal root segments than in younger distal segments that result from aging of root tissues make that the underestimation of the root water uptake redistribution by the parallel root system model is not so important. Even the redistribution of the uptake along a single long root with age dependent root segment conductances can be represented well with a parallel root system model that uses the exact K_{rs} and **SUF**. The big root model overestimates the root water uptake redistribution. But, the estimated root water uptake profiles by this model seem to be affected more by the approximate estimation of K_{rs} and **SUF** from the root segment hydraulic properties. We therefore conclude that bottom-up approaches that start from 3D root architecture models and that use age dependent and/or root order dependent hydraulic properties of root segments are promising approaches to parameterize root water uptake modules of LSMs or crop models. This approach is more reliable than the top-down approach that starts from an upscaled root water uptake model (big root or parallel root model) and derives the effective parameters of these models from root segment hydraulic properties. Since we used information about root segment hydraulic properties and their orientation, the top-down estimated parameters will deviate even more from the correct parameters when proxies of the hydraulic RSA, which are mostly limited to root length density distributions, are used. An often used argument against RSA models and the proposed bottom-up approach, is that they require a lot of input parameters which are hardly available. Indeed, root density distributions are mostly the only information that is available about the RSA. However, root distributions could be used to constrain parameters (Garré et al., 2012;Vansteenkiste et al., 2014) or parameters groups (Pages et al., 2012;Morandage et al., 2019) of RSA models. When information about distributions of root types with depth is available, this information could be used as well to parameterize root architecture models, which provides additional information about the distribution of root segment hydraulic properties when different root types can be associated with different hydraulic properties (De Bauw et al., 2020). Since root architecture models also simulate root growth, they provide information about root segment age, which is related to root hydraulic properties and how they change over time. Root growth but also decay can be modeled as a function of soil properties and soil conditions (e.g. water content) so that the adaptation of root systems to environmental conditions and two-way feedbacks between root system dynamics and soil water content could be represented (Somma et al., 1998). Next to the RSA architecture, also information about the root segment hydraulic properties is required. Overviews of hydraulic properties of different crops, herbaceous species, and trees are given in Bouda et al. (2018) and Draye et al. (2010). But, variations of root hydraulic properties between different root orders or with root age can be very large (Rewald et al., 2011). Root segment hydraulic properties could be derived either from: direct measurements on root segments (Schneider et al., 2017;Zhu and Steudle, 1991;Meunier et al., 2018b); using information on water fluxes in the soil-plant system (e.g. water contents, collar water hydraulic heads, stable water isotopes in the soil and plant xylem) in combination with inverse modeling (Rothfuss and Javaux, 2017;Cai et al., 2018;Meunier et al., 2018a;Couvreur et al., 2020), or using anatomical information about root tissues in combination with flow modeling (Couvreur et al., 2018;Heymans et al., 2020). The latter approach implies a further downscaling to tissue and cellular levels, which could be used to characterize the variability of root segment properties efficiently. A framework for such a multi-scale approach is presented in Passot et al. (2018). With stochastic simulations of hydraulic RSAs, the impact of the variability of root segment properties on root system scale properties and upscaled root water uptake could be derived using the approach presented in this paper.

The uptake profiles and their approximations by the simplified models were calculated for a given non-uniform soil water hydraulic head distribution. Even though the approximations of the uptake profiles are very good, it still requires testing how this evolves over time and affects the dynamics of root water uptake.

The upscaled root water uptake model was derived for a RSA of a single plant or species. The uptake by several plants from the same or from different species of which the roots share the same soil profile with the same $\mathbf{H_{soil}}$ could be represented by summing up the uptake profiles of the individual plants. When the uptake can be described by a parallel root model, Eq. [22], the uptake by a mixture of plants can also be described by an equivalent parallel root model when the $\mathbf{SUF}$s of the different plants are the same. From Eq. [22], it follows that the equivalent K_{rs} for the mixture corresponds with the sum of the K_{rs} values of the individual plants and the equivalent collar hydraulic head with the K_{rs} weighted H_{collar} of the different plants. The joint distribution of K_{rs} and H_{collar} or of K_{rs} and the plant transpiration are required to calculate this weighted mean. For a mixture of plants with a different $\mathbf{SUF}$, it is not possible to derive such an equivalent parallel root model that describes the root water uptake profile of the mixture. In that case, the root water uptake profile should be calculated separately for each species, or 'plant functional' type which is characterized by a specific $\mathbf{SUF}$.

In the current study, we considered a linear flow model in the root system (i.e. root segment hydraulic conductances are not a function of the water pressure heads). Cavitation in the root xylem or changes in radial conductances due to for instance aquaporin activation are not considered. Since we focussed on the root system hydraulic architecture, we did not consider water potential gradients in the rhizosphere between the bulk soil and the soil-root interface. These gradients can be important and generate an additional non-linear resistance to radial flow. It is still debated whether root xylem cavitation or rhizosphere resistance triggers the non-linear system behavior but there seems to be more and more evidence that rhizosphere properties trigger the non-linear behavior of the soil-root system (Carminati et al., 2020). Most root water uptake modules that consider root hydraulics in LSMs already include non-linear rhizosphere resistances. How the root water uptake model and its upscaled and simplified versions that are based on a bottom-up analysis of the hydraulic root architecture can be coupled with approaches that consider non-linear resistances to radial flow in the soil (e.g. (Gardner and Ehlig, 1962;Hillel et al., 1976;de Jong van Lier et al., 2008;de Jong van Lier et al., 2013)) requires further research. Different proposals were made and implemented by (Couvreur et al., 2014b;Meunier et al., 2018a) but a crucial aspect is how these approaches can be scaled up to 1D models. The nonlinearities render the diagonal conductivity matrix $diag(\mathbf{K})$ a function of the hydraulic heads H_{collar}, H_x and H_{soil}. This implies that the full set of (non-linear) equations must be solved iteratively to derive 'exact' upscaled root system properties, K_{rs}, $\mathbf{SUF}$ every time H_{collar}, H_x and H_{soil} change. For large root systems, this approach would be unfeasible so that approximations are required. One approach would be to derive functional relations between the upscaled properties and hydraulic head distributions, root and soil hydraulic properties, and root architectures based on a large set of simulations and advanced data analytics. Another approach would be to start with simplifying assumptions that reduce the complexity of the system. A simplification that we are currently testing exploits the linear behavior of the root hydraulics for upscaling RSA first, using the approach developed in this paper, and couple the upscaled equations subsequently to a non-linear rhizosphere flow model.

6   Appendix

For a given root node i in the discretized root network, the mass balance is:

$$K_x[i]\left(H_x[i]-H_x\big[prox(i)\big]\right)-\sum_{j\in distal(i)}K_x[j]\left(H_x[j]-H_x[i]\right)$$

$$-K_r[i]\left(H_{soil}[i]-H_x[i]\right)=0$$

[A 1]

where *prox(i)* represents the proximal (closer to the collar) node of the segment connected to node *i* and distal(*i*) the distal (further from the collar) node of a segment that is connected to *i*. Note that $H_x\big[prox(i)\big]$ may also be H_{collar} when node *i* is connected to the root collar. The flow from a soil node *i* to xylem node *i* is:

$$K_r[i]\left(H_{soil}[i]-H_x[i]\right)=Q[i]$$

[A 2]

The flow from the collar node is the transpiration rate *T*:

$$-\sum_{j\in distal(collar)}K_x[j]\left(H_x[j]-H_{collar}\right)=-T$$

[A 3]

When we define *dH[i]* as the difference between the pressure head of node *i*, which can also be a soil node, and its proximal node (note that each node is connected to only one proximal node, except the collar which has no proximal node), then it follows that:

$$\mathbf{IM}\cdot diag(\mathbf{K})\cdot\mathbf{dH}=\begin{bmatrix}-T\\\mathbf{0}\\\mathbf{Q}\end{bmatrix}$$

[A 4]

where **IM** is incidence matrix. The differences in pressure heads **dH** can be expressed as:

$$\mathbf{dH}=\mathbf{IM^T}\begin{bmatrix}H_{collar}\\\mathbf{H_x}\\\mathbf{H_{soil}}\end{bmatrix}$$

[A 5]

Plugging Eq. [A 5] in Eq. [A 4] leads to Eq. [4].

When the transpiration *T* and **H_soil** are known, H_{collar} and **H_x** can be obtained by solving the first $N_{root}+1$ equations of Eq. [4]. Alternatively, H_{collar} can be obtained directly from Eq. [6]. From H_{collar} and **H_soil**, **H_x** can be derived from solving the 2nd to $N_{root}+1$ equations in Eq. [4]. The xylem hydraulic heads are obtained from:

$$H_{collar}\mathbf{C_1}+\mathbf{C_2}\mathbf{H_x}+\mathbf{C_3}\mathbf{H_{soil}}=\mathbf{0}$$
$$\mathbf{H_x}=-\mathbf{C_2}^{-1}\left[\mathbf{C_3}\mathbf{H_{soil}}+H_{collar}\mathbf{C_1}\right]$$

[A 6]

where

$$\mathbf{C}=\mathbf{IM}\cdot diag(\mathbf{K})\cdot\mathbf{IM_{collar}^T}$$

[A 7]

$\mathbf{C_1}=C[i,j]\ for\ i=2,...,N_{root}+1,\ j=1$ $C_1[i]=-K_x[i]\quad if\quad prox(i)=collar$ [A 8]

$\mathbf{C_2}=C[i,j]$ $C_2[i,i]=K_x[i]+\sum_{j\in distal(i)}K_x[j]+K_r[i]$ [A 9]

for i=2,...,N_root+1, j=2,...,N_root+1

$C_2[i,j]=-K_x[i]\quad if\quad prox(i)=j$

$C_2[i,j]=-K_x[j]\quad if\quad j\in distal(i)$

$\mathbf{C_3}=C[i,j]$ $C_3[i,i+N_{root}]=-K_r[i]$ [A 10]

for i=2,...,N_root+1, j= N_root+2,...,2N_root+1

Note that $\mathbf{C_2}$ and $\mathbf{C_3}$ are symmetric matrices.

For the fluxes, we can write using the lower part of the **C** matrix that:

$$\mathbf{Q} = C\left[i = N_{root} + 2, ..., 2N_{root} + 1, j = 1, ..., 2N_{root} + 1\right] \begin{bmatrix} H_{collar} \\ \mathbf{H_x} \\ \mathbf{H_{soil}} \end{bmatrix} \qquad \text{[A 11]}$$

This can be written out as:

$$\mathbf{Q} = \mathbf{C_{L1}} H_{collar} + \mathbf{C_{L2}} \mathbf{H_x} + \mathbf{C_{L3}} \mathbf{H_{soil}} \qquad \text{[A 12]}$$

655   where

$$\mathbf{C_{L1}} = C[i, j] \ for \ i = N_{root} + 2, ..., 2N_{root} + 1, j = 1 \qquad \text{[A 13]}$$

$$\mathbf{C_{L2}} = C[i, j] \ for \ i = N_{root} + 2, ..., 2N_{root} + 1, j = 2, ..., N_{root} + 1 \qquad \text{[A 14]}$$

$$\mathbf{C_{L3}} = C[i, j] \ for \ i = N_{root} + 2, ..., 2N_{root} + 1, j = N_{root} + 2, ..., 2N_{root} + 1 \qquad \text{[A 15]}$$

working out Eq. [A 7], it is found that all entries in $\mathbf{C_{L1}}$ are 0, $\mathbf{C_{L2}} = $ -diag($\mathbf{K_r}$) and $\mathbf{C_{L3}} = $ diag($\mathbf{K_r}$), so that Eq. [A 12] corresponds with:

$$\mathbf{Q} = diag(\mathbf{K_r})\left[\mathbf{H_{soil}} - \mathbf{H_x}\right] \qquad \text{[A 16]}$$

which is the matrix form of Eq. [A 2]. Plugging Eq. [A 6] into the general form of Eq. [A 12] gives:

$$\mathbf{C_4} \mathbf{H_{soil}} + \mathbf{C_5} H_{collar} = \mathbf{Q} \quad \left(N_{root} \, x \, 1\right) \qquad \text{[A 17]}$$

where

$$\mathbf{C_4} = -\mathbf{C_{L2}} \mathbf{C_2^{-1}} \mathbf{C_3} + \mathbf{C_{L3}} \qquad \text{[A 18]}$$

$$\mathbf{C_5} = \mathbf{C_{L1}} - \mathbf{C_{L2}} \mathbf{C_2^{-1}} \mathbf{C_1} \qquad \text{[A 19]}$$

660   Note that since $\mathbf{C_2}$ and $\mathbf{C_3}$ are symmetric matrices, also $\mathbf{C_4}$ is a symmetric matrix and **C4** and C5 simplify due to the simple forms of $\mathbf{C_{L1}}$, $\mathbf{C_{L2}}$, and $\mathbf{C_{L3}}$:

$$\mathbf{C_4} = diag(\mathbf{K_r})\left[\mathbf{I} + \mathbf{C_2^{-1}} \mathbf{C_3}\right] \quad \left(N_{root} \, x N_{root}\right) \qquad \text{[A 20]}$$

$$\mathbf{C_5} = diag(\mathbf{K_r})\mathbf{C_2^{-1}} \mathbf{C_1} \quad \left(N_{root} \, x \, 1\right) \qquad \text{[A 21]}$$

When we consider the case of a uniform soil hydraulic head, H_{eff}, then we can write

$$Q[i] = H_{eff} \sum_j C_4[i, j] + H_{collar} C_5[i] \qquad \text{[A 22]}$$

When $H_{eff} = H_{collar}$, there is neither flow from the soil to the collar nor flow through the root system from one soil node to the other. From this follows that:

$$\sum_j C_4[i, j] = -C_5[i] \qquad \text{[A 23]}$$

665   If we consider now the total root water uptake, Q_{tot}, which is equal to the transpiration rate, T, then

$$Q_{tot} = \sum_i Q[i] = -\sum_i C_5[i]\left(H_{eff} - H_{collar}\right) \qquad \text{[A 24]}$$

From this follows that we can derive the root system conductance K_{rs} directly from:

$$K_{rs} = \frac{Q_{tot}}{\left(H_{eff} - H_{collar}\right)} \qquad \text{[A 25]}$$

$$K_{rs} = -\sum_i C_5[i] = \sum_i \sum_j C_4[i, j]$$

The standardized uptake fraction $SUF[i]$, which is defined as the fraction of the uptake by a root node to the total root water uptake under uniform soil water hydraulic head, is related to the matrix $\mathbf{C_4}$ and vector $\mathbf{C_5}$ as:

$$SUF[i] = \frac{Q[i]}{Q_{tot}} = \frac{\sum_j C_4[i,j]}{\sum_i \sum_j C_4[i,j]} = \frac{C_5[i]}{\sum_i C_5[i]} \qquad [A\ 26]$$

So we can write for uniform soil water hydraulic heads:

$$Q[i] = K_{rs} SUF[i]\left(H_{eff} - H_{collar}\right) \qquad [A\ 27]$$

670 For the general case that the soil water hydraulic heads are not uniform, we can define the effective soil water hydraulic head, H_{eff}, as:

$$H_{eff} = \mathbf{SUF}^T \mathbf{H_{soil}} \qquad [A\ 28]$$

After adding and subtracting $\mathbf{C_5}\,H_{eff} = K_{rs}\,\mathbf{SUF}\,H_{eff} = K_{rs}\,\mathbf{SUF}\cdot\mathbf{SUF}^T\,\mathbf{H_{soil}}$ in Eq. [A 17], we obtain the following equation for the root water uptake $\mathbf{Q}$:

$$\mathbf{Q} = K_{rs}\mathbf{SUF}\left(H_{eff} - H_{collar}\right) + \mathbf{C_6}\mathbf{H_{soil}} \qquad [A\ 29]$$

$$\mathbf{C_6} = \mathbf{C_4} - K_{rs}\mathbf{SUF}\cdot\mathbf{SUF}^T \qquad [A\ 30]$$

675 From the definitions of $\mathbf{C_6}$, $\mathbf{C_4}$, $\mathbf{SUF}$ and K_{rs} follows that the sum of the elements in the rows of $\mathbf{C_6}$ is zero for all rows. This implies that when $\mathbf{C_6}$ is multiplied with an N_{root} x 1 vector with constant elements, a zero vector is obtained. Therefore, we can reformulate the equation for the root water uptake as:

$$\mathbf{Q} = K_{rs}\mathbf{SUF}\left(H_{eff} - H_{collar}\right) + \mathbf{C_6}\left(\mathbf{H_{soil}} - \mathbf{H_{eff}}\right) \qquad [A\ 31]$$

Since $\mathbf{SUF^T}\,\mathbf{H_{soil}} = H_{eff}$ and since the sum of all elements in $\mathbf{SUF}$ is one so that $\mathbf{SUF^T}\,\mathbf{H_{eff}} = H_{eff}$, it follows also that:

$$\mathbf{Q} = K_{rs}\mathbf{SUF}\left(H_{eff} - H_{collar}\right) + \mathbf{C_4}\left(\mathbf{H_{soil}} - \mathbf{H_{eff}}\right) \qquad [A\ 32]$$

The definition of H_{eff} (Eq. [A 28]) makes that sums of all the fluxes in the second term of Eq. [A 31] and in the second term

680 of Eq. [A 32] are both zero. Indeed, when considering Eq. [A 32], we can write:

$$[A\ 33]$$

$$\sum_i \sum_j C_4[i,j]H_{soil}[j] - \sum_i\left(\sum_j C_4[i,j]\right)\left(\sum_i SUF[i]H_{soil}[i]\right)$$

$$= \sum_i \sum_j C_4[i,j]H_{soil}[j] - \sum_i \sum_j C_4[i,j]\left(\frac{\sum_i \sum_j C_4[i,j]H_{soil}[i]}{\sum_i \sum_j C_4[i,j]}\right)$$

$$= \sum_i \sum_j C_4[i,j]H_{soil}[j] - \sum_i \sum_j C_4[i,j]H_{soil}[i]$$

$$= 0$$

since $C_4[i,j] = C_4[j,i]$

Eqs. [A 31] and [A 32] have a similar form as the equation that was proposed by Couvreur et al. (2012) to describe water uptake by a root network. In order to draw the analogy and identify differences between the two approaches, we will discuss the nature of the $\mathbf{C_6}$ matrix and how it can be transformed or approximated. From the definition of $\mathbf{C_6}$, it also follows that the

685 sum of all the elements in the vector $\mathbf{C_6}\left(\mathbf{H_{soil}} - \mathbf{H_{eff}}\right)$ is zero. Therefore, this vector represents the perturbations of the

uptake $\Delta\mathbf{Q}$ at a certain depth due to the perturbation of the soil water hydraulic head at this depth compared to the uptake when the soil water hydraulic head is uniform in the root zone. When there is no net uptake, i.e. when $H_{eff} = H_{collar}$, then $\mathbf{C_6}\left(\mathbf{H_{soil}} - \mathbf{H_{eff}}\right)$ represents the redistribution water fluxes through the root system due to spatial variations in $\mathbf{H_{soil}}$. When we consider now that the soil water hydraulic head around node i is ΔH higher than the hydraulic head in all other nodes, then we can define $\Delta Q[i] = k_{comp}[i]\, \Delta H$. $k_{comp}[i]$ represents the compensatory root system conductance to transfer water from node i towards all other nodes when there is a hydraulic head difference between the soil water at node i and the soil water next to all other nodes in the root system. $\Delta Q[i]$ and $k_{comp}[i]$ are related to the $\mathbf{C_6}$ matrix and $\mathbf{SUF}$ vector as:

$$\Delta Q[i] = \left(\left(1 - SUF[i]\right) C_6[i,i] - SUF[i] \sum_{j \neq i} C_6[i,j] \right) \Delta H \qquad \text{[A 34]}$$

$$k_{comp}[i] = \frac{\Delta Q[i]}{\Delta H} = \left(\left(1 - SUF[i]\right) C_6[i,i] - SUF[i] \sum_{j \neq i} C_6[i,j] \right) = C_6[i,i] \qquad \text{[A 35]}$$

since

$$C_6[i,i] + \sum_{j \neq i} C_6[i,j] = 0 \qquad \text{[A 36]}$$

We assume now a root system in which all soil nodes are connected via one radial and one axial resistance to the collar node so that the overall resistance to flow from one soil-root node to the collar is equal to the sum of the axial plus radial resistances. We call this root system the 'parallel root system'. The radial and axial resistances for each soil node can however be different. Also a root system in which there is no resistance to axial flow can be considered as a system in which all soil nodes are connected directly to the root collar. But, it is important to keep in mind that systems with a significant axial root resistance can also be considered, as long as there is a direct connection between the soil node and the root collar without additional intermediate nodes that connect to the soil. For instance, fibrous root systems with only primary roots, in which uptake takes only place near the root tip but not at the more basal ends, can also be represented by this root system model. For such a root system, it follows that:

$$k_{comp}[i] = SUF[i]\left(1 - SUF[i]\right) K_{rs} \qquad \text{[A 37]}$$

In the same vein, it can be deduced that for such a parallel root system:

$$\frac{C_6[i,j]}{C_6[i,i]} = -\frac{SUF[j]}{\left(1 - SUF[i]\right)} \quad \text{for } i \neq j \qquad \text{[A 38]}$$

The jth column of the $\mathbf{C_6}$ matrix represents to what extent water from the jth node can flow to the other nodes in the system. For a parallel root system, in which the flow must pass through the collar node, the flow from node j to node i is proportional to the conductance for the flow from node j to the collar node and hence to $SUF[j]$. Based on this, we can write the $\mathbf{C_6}$ matrix for this root system as:

$$\mathbf{C_6} = diag\left(\frac{C_6[i,i]}{1 - SUF[i]} \right)\left(\mathbf{I} - \mathbf{ones} \cdot \mathbf{SUF^T} \right) = K_{rs}\, diag\left(SUF[i] \right)\left(\mathbf{I} - \mathbf{ones} \cdot \mathbf{SUF^T} \right) \qquad \text{[A 39]}$$

where $\mathbf{ones}$ is the N_{root} all-ones vector.

Since $\mathbf{SUF^T}\, \mathbf{H_{soil}} = \mathbf{SUF^T}\, \mathbf{H_{eff}} = \mathbf{H_{eff}}$, it follows that for a parallel root system:

$$\mathbf{C_6}\left(\mathbf{H_{soil}} - \mathbf{H_{eff}} \right) = K_{rs}\, diag\left(\mathbf{SUF} \right)\left(\mathbf{H_{soil}} - \mathbf{H_{eff}} \right) \qquad \text{[A 40]}$$

This implies that we can obtain the following equation to simulate root water uptake for the parallel root system:

$$\mathbf{Q} = K_{rs}\mathbf{SUF}\left(H_{eff} - H_{collar} \right) + K_{rs}\, diag\left(\mathbf{SUF} \right)\left(\mathbf{H_{soil}} - \mathbf{H_{eff}} \right) \qquad \text{[A 41]}$$

which is identical to the equation proposed by Couvreur et al. (2012).

For a general root system, we can rewrite the general equation which takes a similar form as the equation that we obtained for the parallel root system.

$$\mathbf{Q} = K_{rs}\mathbf{SUF}\left(H_{eff} - H_{collar}\right) + diag\left(\mathbf{K_{comp}}\right)diag\left(\mathbf{SUF}\right)\mathbf{C_7}\left(\mathbf{H_{soil}} - \mathbf{H_{eff}}\right) \qquad \text{[A 42]}$$

$$K_{comp}\left[i\right] = \frac{C_6\left[i,i\right]}{SUF\left[i\right]\left(1 - SUF\left[i\right]\right)} = \frac{k_{comp}\left[i\right]}{SUF\left[i\right]\left(1 - SUF\left[i\right]\right)} \qquad \text{[A 43]}$$

$$\mathbf{C_7} = diag\left(\frac{\left(1 - SUF\left[i\right]\right)}{C_6\left[i,i\right]}\right)\mathbf{C_6} + \mathbf{ones} \cdot \mathbf{SUF^T} \qquad \text{[A 44]}$$

For the parallel root system, $\mathbf{C_7}$ equals the identity matrix and $K_{comp}[i]$ equals K_{rs}.

715

7   Author contributions:

VC initiated the study on the exact macroscopic representation and upscaling of root water uptake. Model development was done by JV, VC, FM, MJ, and MB and programming was done by JV, VC and FM. Codes were checked by AS. All authors contributed to the conceptualization of the paper. JV wrote the paper, which was critically reviewed by all co-authors.

720

8   Acknowledgements

We would like to thank the reviewers whose comments helped us to improve the paper.

This work has partially been funded by the German Research Foundation under Germany's Excellence Strategy, EXC-2070 – 390732324 – PhenoRob and in the framework of projects P3 and P24 of the priority programme 2089 'Rhizosphere spatiotemporal organization – a key to rhizosphere functions'. VC was supported by the Belgian National Fund for Scientific Research (FRS-FNRS; grant no. 1208619F), the Interuniversity Attraction Poles Program of the Belgian Science Policy Office (grant no. IAP7/29) and the Communauté française de Belgique-Actions de Recherches Concertées (grant no. ARC16/21-075), the EPPN2020 731013 and EMPHASIS-PREP 739514 projects. MB was supported by long-term research development project No. RVO 67985939 of the Czech Academy of Sciences and the project CZ.02.2.69/0.0/0.0/18_070/0009075 of the Czech Ministry of Education (OP RDE).

725

730

8.1 References

Amenu, G. G., and Kumar, P.: A model for hydraulic redistribution incorporating coupled soil-root moisture transport, Hydrology and Earth System Sciences, 12, 55-74, 10.5194/hess-12-55-2008, 2008.

Bouda, M., and Saiers, J. E.: Dynamic effects of root system architecture improve root water uptake in 1D process-based soil-root hydrodynamics, Adv. Water Resour., 110, 319-334, 10.1016/j.advwatres.2017.10.018, 2017.

Bouda, M., Brodersen, C., and Saiers, J.: Whole root system water conductance responds to both axial and radial traits and network topology over natural range of trait variation, J. Theor. Biol., 456, 49-61, 10.1016/j.jtbi.2018.07.033, 2018.

Bouda, M.: A Big Root Approximation of Site-Scale Vegetation Water Uptake, Journal of Advances in Modeling Earth Systems, 11, 4597–4613, 10.1029/2019ms001806, 2019.

Cai, G. C., Vanderborght, J., Couvreur, V., Mboh, C. M., and Vereecken, H.: Parameterization of Root Water Uptake Models Considering Dynamic Root Distributions and Water Uptake Compensation, Vadose Zone J., 17, 10.2136/vzj2016.12.0125, 2018.

Carminati, A., Ahmed, M. A., Zarebanadkouki, M., Cai, G., Lovric, G., and Javaux, M.: Stomatal closure prevents the drop in soil water potential around roots, New Phytol., 226, 1541-1543, https://doi.org/10.1111/nph.16451, 2020.

Couvreur, V., Vanderborght, J., and Javaux, M.: A simple three-dimensional macroscopic root water uptake model based on the hydraulic architecture approach, Hydrol. Earth Syst. Sci., 16, 2957-2971, 10.5194/hess-16-2957-2012, 2012.

Couvreur, V., Vanderborght, J., Beff, L., and Javaux, M.: Horizontal soil water potential heterogeneity: simplifying approaches for crop water dynamics models, Hydrol. Earth Syst. Sci., 18, 1723-1743, 10.5194/hess-18-1723-2014, 2014a.

Couvreur, V., Vanderborght, J., Draye, X., and Javaux, M.: Dynamic aspects of soil water availability for isohydric plants: Focus on root hydraulic resistances, Water Resour. Res., 50, 8891-8906, 10.1002/2014wr015608, 2014b.

Couvreur, V., Faget, M., Lobet, G., Javaux, M., Chaumont, F., and Draye, X.: Going with the Flow: Multiscale Insights into the Composite Nature of Water Transport in Roots, Plant Physiol., 178, 1689-1703, 10.1104/pp.18.01006, 2018.

Couvreur, V., Rothfuss, Y., Meunier, F., Bariac, T., Biron, P., Durand, J. L., Richard, P., and Javaux, M.: Disentangling temporal and population variability in plant root water uptake from stable isotopic analysis: when rooting depth matters in labeling studies, Hydrology and Earth System Sciences, 24, 3057-3075, 10.5194/hess-24-3057-2020, 2020.

Daly, K. R., Tracy, S. R., Crout, N. M. J., Mairhofer, S., Pridmore, T. P., Mooney, S. J., and Roose, T.: Quantification of root water uptake in soil using X-ray computed tomography and image-based modelling, Plant Cell Environ, 41, 121-133, 10.1111/pce.12983, 2018.

De Bauw, P., Mai, T. H., Schnepf, A., Merckx, R., Smolders, E., and Vanderborght, J.: A functional-structural model of upland rice root systems reveals the importance of laterals and growing root tips for phosphate uptake from wet and dry soils, Ann. Bot., 126, 789-806, 10.1093/aob/mcaa120, 2020.

de Jong van Lier, Q., van Dam, J. C., Durigon, A., dos Santos, M. A., and Metselaar, K.: Modeling Water Potentials and Flows in the Soil–Plant System Comparing Hydraulic Resistances and Transpiration Reduction Functions, Vadose Zone J., 12, 10.2136/vzj2013.02.0039, 2013.

de Jong van Lier, Q. D., van Dam, J. C., Metselaar, K., de Jong, R., and Duijnisveld, W. H. M.: Macroscopic root water uptake distribution using a matric flux potential approach, Vadose Zone J., 7, 1065-1078, 10.2136/vzj2007.0083, 2008.

Doussan, C., Pages, L., and Vercambre, G.: Modelling of the hydraulic architecture of root systems: An integrated approach to water absorption - Model description, Ann. Bot., 81, 213-223, 1998.

Doussan, C., Pierret, A., Garrigues, E., and Pages, L.: Water uptake by plant roots: II - Modelling of water transfer in the soil root-system with explicit account of flow within the root system - Comparison with experiments, Plant Soil, 283, 99-117, 2006.

Draye, X., Kim, Y., Lobet, G., and Javaux, M.: Model-assisted integration of physiological and environmental constraints affecting the dynamic and spatial patterns of root water uptake from soils, J. Exp. Bot., 61, 2145-2155 10.1093/jxb/erq077, 2010.

785 Feddes, R. A., Hoff, H., Bruen, M., Dawson, T., de Rosnay, P., Dirmeyer, O., Jackson, R. B., Kabat, P., Kleidon, A., Lilly, A., and Pitman, A. J.: Modeling root water uptake in hydrological and climate models, Bull. Amer. Meteorol. Soc., 82, 2797-2809, 2001.

Ferguson, I. M., Jefferson, J. L., Maxwell, R. M., and Kollet, S. J.: Effects of root water uptake formulation on simulated water and energy budgets at local and basin scales, Environ. Earth Sci., 75, 10.1007/s12665-015-
790 5041-z, 2016.

Fu, C. S., Wang, G. L., Goulden, M. L., Scott, R. L., Bible, K., and Cardon, Z. G.: Combined measurement and modeling of the hydrological impact of hydraulic redistribution using CLM4.5 at eight AmeriFlux sites, Hydrology and Earth System Sciences, 20, 2001-2018, 10.5194/hess-20-2001-2016, 2016.

Gardner, W. R., and Ehlig, C. F.: SOME OBSERVATIONS ON MOVEMENT OF WATER TO PLANT ROOTS, Agron. J.,
795 54, 453-&, 10.2134/agronj1962.00021962005400050024x, 1962.

Garré, S., Pagès, L., Laloy, E., Javaux, M., Vanderborght, J., and Vereecken, H.: Parameterizing a Dynamic Architectural Model of the Root System of Spring Barley from Minirhizotron Data, Vadose Zone J., 11, 10.2136/vzj2011.0179, 2012.

Gayler, S., Ingwersen, J., Priesack, E., Wohling, T., Wulfmeyer, V., and Streck, T.: Assessing the relevance of
800 subsurface processes for the simulation of evapotranspiration and soil moisture dynamics with CLM3.5: comparison with field data and crop model simulations, Environ. Earth Sci., 69, 415-427, 10.1007/s12665-013-2309-z, 2013.

Good, S. P., Noone, D., and Bowen, G.: Hydrologic connectivity constrains partitioning of global terrestrial water fluxes, Science, 349, 175-177, 10.1126/science.aaa5931, 2015.

805 Gou, S., and Miller, G.: A groundwater-soil-plant-atmosphere continuum approach for modelling water stress, uptake, and hydraulic redistribution in phreatophytic vegetation, Ecohydrology, 7, 1029-1041, 10.1002/eco.1427, 2014.

Heymans, A., Couvreur, V., LaRue, T., Paez-Garcia, A., and Lobet, G.: GRANAR, a Computational Tool to Better Understand the Functional Importance of Monocotyledon Root Anatomy, Plant Physiol., 182, 707-720,
810 10.1104/pp.19.00617, 2020.

Hillel, D., Talpaz, H., and Vankeulen, H.: MACROSCOPIC-SCALE MODEL OF WATER UPTAKE BY A NONUNIFORM ROOT-SYSTEM AND OF WATER AND SALT MOVEMENT IN SOIL PROFILE, Soil Sci., 121, 242-255, 10.1097/00010694-197604000-00009, 1976.

Hopmans, J. W., and Bristow, K. L.: Current capabilities and future needs of root water and nutrient uptake
815 modeling, in: Advances in Agronomy, Vol 77, Advances in Agronomy, 103-183, 2002.

Jarvis, N. J.: Simple physics-based models of compensatory plant water uptake: concepts and eco-hydrological consequences, Hydrol. Earth Syst. Sci., 15, 3431-3446, 10.5194/hess-15-3431-2011, 2011.

Javaux, M., Schröder, T., Vanderborght, J., and Vereecken, H.: Use of a three-dimensional detailed modeling approach for predicting root water uptake, Vadose Zone J., 7, 1079-1088, 10.2136/vzj2007.0115, 2008.

820 Javaux, M., Couvreur, V., Vanderborght, J., and Vereecken, H.: Root Water Uptake: From Three-Dimensional Biophysical Processes to Macroscopic Modeling Approaches, Vadose Zone J., 12, -, 10.2136/vzj2013.02.0042, 2013.

Katul, G. G., and Siqueira, M. B.: Biotic and abiotic factors act in coordination to amplify hydraulic redistribution and lift, New Phytol., 187, 4-6, 2010.

825 Kennedy, D., Swenson, S., Oleson, K. W., Lawrence, D. M., Fisher, R., da Costa, A. C. L., and Gentine, P.: Implementing Plant Hydraulics in the Community Land Model, Version 5, Journal of Advances in Modeling Earth Systems, 11, 485-513, 10.1029/2018ms001500, 2019.

Landsberg, J. J., and Fowkes, N. D.: WATER-MOVEMENT THROUGH PLANT ROOTS, Ann. Bot., 42, 493-508, 10.1093/oxfordjournals.aob.a085488, 1978.

830 Liu, Y., Kumar, M., Katul, G. G., Feng, X., and Konings, A. G.: Plant hydraulics accentuates the effect of atmospheric moisture stress on transpiration, Nature Climate Change, 10, 691-695, 10.1038/s41558-020-0781-5, 2020.

Manoli, G., Bonetti, S., Domec, J. C., Putti, M., Katul, G., and Marani, M.: Tree root systems competing for soil moisture in a 3D soil-plant model, Adv. Water Resour., 66, 32-42, 10.1016/j.advwatres.2014.01.006, 2014.

835 Manoli, G., Huang, C. W., Bonetti, S., Domec, J. C., Marani, M., and Katul, G.: Competition for light and water in a coupled soil-plant system, Adv. Water Resour., 108, 216-230, 10.1016/j.advwatres.2017.08.004, 2017.

Meunier, F., Couvreur, V., Draye, X., Vanderborght, J., and Javaux, M.: Towards quantitative root hydraulic phenotyping: novel mathematical functions to calculate plant-scale hydraulic parameters from root system functional and structural traits, J. Math. Biol., 75, 1133-1170, 10.1007/s00285-017-1111-z, 2017a.

840   Meunier, F., Couvreur, V., Draye, X., Zarebanadkouki, M., Vanderborght, J., and Javaux, M.: Water movement through plant roots - exact solutions of the water flow equation in roots with linear or exponential piecewise hydraulic properties, Hydrol. Earth Syst. Sci., 21, 6519-6540, 10.5194/hess-21-6519-2017, 2017b.

Meunier, F., Draye, X., Vanderborght, J., Javaux, M., and Couvreur, V.: A hybrid analytical-numerical method for solving water flow equations in root hydraulic architectures, Appl. Math. Model., 52, 648-663,
845   10.1016/j.apm.2017.08.011, 2017c.

Meunier, F., Rothfuss, Y., Bariac, T., Biron, P., Richard, P., Durand, J. L., Couvreur, V., Vanderborght, J., and Javaux, M.: Measuring and Modeling Hydraulic Lift of Lolium multiflorum Using Stable Water Isotopes, Vadose Zone J., 17, 10.2136/vzj2016.12.0134, 2018a.

Meunier, F., Zarebanadkouki, M., Ahmed, M. A., Carminati, A., Couvreur, V., and Javaux, M.: Hydraulic
850   conductivity of soil-growth lupine and maize unbranched roots and maize root-shoot junctions, J. Plant Physiol., 227, 31-44, 10.1016/j.jplph.2017.12.019, 2018b.

Morandage, S., Schnepf, A., Leitner, D., Javaux, M., Vereecken, H., and Vanderborght, J.: Parameter sensitivity analysis of a root system architecture model based on virtual field sampling, Plant Soil, 10.1007/s11104-019-03993-3, 2019.

855   Nguyen, T. H., Langensiepen, M., Vanderborght, J., Hüging, H., Mboh, C. M., and Ewert, F.: Comparison of root water uptake models in simulating CO_2 and H_2O fluxes and growth of wheat, Hydrol. Earth Syst. Sci., 24, 4943-4969, 10.5194/hess-24-4943-2020, 2020.

Nimah, M. N., and Hanks, R. J.: MODEL FOR ESTIMATING SOIL-WATER, PLANT, AND ATMOSPHERIC INTERRELATIONS .1. DESCRIPTION AND SENSITIVITY, Soil Sci. Soc. Am. J., 37, 522-527,
860   10.2136/sssaj1973.03615995003700040018x, 1973.

Oki, T., and Kanae, S.: Global Hydrological Cycles and World Water Resources, Science, 313, 1068-1072, 10.1126/science.1128845, 2006.

Pages, L., Bruchou, C., and Garre, S.: Links Between Root Length Density Profiles and Models of the Root System Architecture, Vadose Zone J., 11, 10.2136/vzj2011.0152, 2012.

865   Passot, S., Couvreur, V., Meunier, F., Draye, X., Javaux, M., Leitner, D., Pagès, L., Schnepf, A., Vanderborght, J., and Lobet, G.: Connecting the dots between computational tools to analyse soil-root water relations, J. Exp. Bot., ery361-ery361, 10.1093/jxb/ery361, 2018.

Quijano, J. C., Kumar, P., Drewry, D. T., Goldstein, A., and Misson, L.: Competitive and mutualistic dependencies in multispecies vegetation dynamics enabled by hydraulic redistribution, Water Resour. Res., 48,
870   10.1029/2011wr011416, 2012.

Quijano, J. C., Kumar, P., and Drewry, D. T.: Passive regulation of soil biogeochemical cycling by root water transport, Water Resour. Res., 49, 3729-3746, 10.1002/wrcr.20310, 2013.

Quijano, J. C., and Kumar, P.: Numerical simulations of hydraulic redistribution across climates: The role of the root hydraulic conductivities, Water Resour. Res., 51, 8529-8550, 10.1002/2014wr016509, 2015.

875   Rewald, B., Ephrath, J. E., and Rachmilevitch, S.: A root is a root is a root? Water uptake rates of Citrus root orders, Plant Cell Environ., 34, 33-42, 10.1111/j.1365-3040.2010.02223.x, 2011.

Roose, T., and Fowler, A. C.: A model for water uptake by plant roots, J. Theor. Biol., 228, 155-171, 10.1016/j.jtbi.2003.12.012, 2004.

Rothfuss, Y., and Javaux, M.: Reviews and syntheses: Isotopic approaches to quantify root water uptake: a
880   review and comparison of methods, Biogeosciences, 14, 2199-2224, 10.5194/bg-14-2199-2017, 2017.

Ryel, R. J., Caldwell, M. M., Yoder, C. K., Or, D., and Leffler, A. J.: Hydraulic redistribution in a stand of Artemisia tridentata: evaluation of benefits to transpiration assessed with a simulation model, Oecologia, 130, 173-184, 10.1007/s004420100794, 2002.

Schneider, H. M., Wojciechowski, T., Postma, J. A., Brown, K. M., Lücke, A., Zeisler, V., Schreiber, L., and Lynch, J.
885   P.: Root cortical senescence decreases root respiration, nutrient content and radial water and nutrient transport in barley, Plant, Cell & Environment, 40, 1392-1408, https://doi.org/10.1111/pce.12933, 2017.

Schnepf, A., Leitner, D., Landl, M., Lobet, G., Mai, T. H., Morandage, S., Sheng, C., Zorner, M., Vanderborght, J., and Vereecken, H.: CRootBox: a structural-functional modelling framework for root systems, Ann. Bot., 121, 1033-1053, 10.1093/aob/mcx221, 2018.

890   Simunek, J., and Hopmans, J. W.: Modeling compensated root water and nutrient uptake, Ecol. Model., 220, 505-521, 10.1016/j.ecolmodel.2008.11.004, 2009.

Siqueira, M., Katul, G., and Porporato, A.: Onset of water stress, hysteresis in plant conductance, and hydraulic lift: Scaling soil water dynamics from millimeters to meters, Water Resour. Res., 44, 10.1029/2007wr006094, 2008.

895   Somma, F., Hopmans, J. W., and Clausnitzer, V.: Transient three-dimensional modeling of soil water and solute transport with simultaneous root growth, root water and nutrient uptake, Plant Soil, 202, 281-293, 1998.

Sulis, M., Couvreur, V., Keune, J., Cai, G., Trebs, I., Junk, J., Shrestha, P., Simmer, C., Kollet, S. J., Vereecken, H., and Vanderborght, J.: Incorporating a root water uptake model based on the hydraulic architecture approach in terrestrial systems simulations, Agricultural and Forest Meteorology, 269-270, 28-45,

900   https://doi.org/10.1016/j.agrformet.2019.01.034, 2019.

Tang, J. Y., Riley, W. J., and Niu, J.: Incorporating root hydraulic redistribution in CLM4.5: Effects on predicted site and global evapotranspiration, soil moisture, and water storage, Journal of Advances in Modeling Earth Systems, 7, 1828-1848, 10.1002/2015ms000484, 2015.

Trenberth, K. E., Smith, L., Qian, T., Dai, A., and Fasullo, J.: Estimates of the Global Water Budget and Its Annual

905   Cycle Using Observational and Model Data, Journal of Hydrometeorology, 8, 758-769, 10.1175/jhm600.1, 2007.

Vansteenkiste, J., Van Loon, J., Garre, S., Pages, L., Schrevens, E., and Diels, J.: Estimating the parameters of a 3-D root distribution function from root observations with the trench profile method: case study with simulated and field-observed root data, Plant Soil, 375, 75-88, 10.1007/s11104-013-1942-3, 2014.

Vereecken, H., Huisman, J. A., Franssen, H. J. H., Bruggemann, N., Bogena, H. R., Kollet, S., Javaux, M., van der

910   Kruk, J., and Vanderborght, J.: Soil hydrology: Recent methodological advances, challenges, and perspectives, Water Resour. Res., 51, 2616-2633, 10.1002/2014wr016852, 2015.

Vereecken, H., Schnepf, A., Hopmans, J. W., Javaux, M., Or, D., Roose, T., Vanderborght, J., Young, M. H., Amelung, W., Aitkenhead, M., Allison, S. D., Assouline, S., Baveye, P., Berli, M., Brüggemann, N., Finke, P., Flury, M., Gaiser, T., Govers, G., Ghezzehei, T., Hallett, P., Hendricks Franssen, H. J., Heppell, J., Horn, R., Huisman, J.

915   A., Jacques, D., Jonard, F., Kollet, S., Lafolie, F., Lamorski, K., Leitner, D., McBratney, A., Minasny, B., Montzka, C., Nowak, W., Pachepsky, Y., Padarian, J., Romano, N., Roth, K., Rothfuss, Y., Rowe, E. C., Schwen, A., Šimůnek, J., Tiktak, A., Van Dam, J., van der Zee, S. E. A. T. M., Vogel, H. J., Vrugt, J. A., Wöhling, T., and Young, I. M.: Modeling Soil Processes: Review, Key Challenges, and New Perspectives, Vadose Zone J., 15, 10.2136/vzj2015.09.0131, 2016.

920   Whitley, R., Beringer, J., Hutley, L. B., Abramowitz, G., De Kauwe, M. G., Evans, B., Haverd, V., Li, L. H., Moore, C., Ryu, Y., Scheiter, S., Schymanski, S. J., Smith, B., Wang, Y. P., Williams, M., and Yu, Q.: Challenges and opportunities in land surface modelling of savanna ecosystems, Biogeosciences, 14, 4711-4732, 10.5194/bg-14-4711-2017, 2017.

Wilderotter, O.: An adaptive numerical method for the Richards equation with root growth, Plant Soil, 251, 255-

925   267, 10.1023/a:1023031924963, 2003.

Wöhling, T., Gayler, S., Priesack, E., Ingwersen, J., Wizemann, H.-D., Högy, P., Cuntz, M., Attinger, S., Wulfmeyer, V., and Streck, T.: Multiresponse, multiobjective calibration as a diagnostic tool to compare accuracy and structural limitations of five coupled soil-plant models and CLM3.5, Water Resour. Res., 49, 8200-8221, 10.1002/2013WR014536, 2013.

930   Yan, B. Y., and Dickinson, R. E.: Modeling hydraulic redistribution and ecosystem response to droughts over the Amazon basin using Community Land Model 4.0 (CLM4), J. Geophys. Res.-Biogeosci., 119, 2130-2143, 10.1002/2014jg002694, 2014.

Zarebanadkouki, M., Meunier, F., Couvreur, V., Cesar, J., Javaux, M., and Carminati, A.: Estimation of the hydraulic conductivities of lupine roots by inverse modelling of high-resolution measurements of root water

935   uptake, Ann. Bot., 118, 853-864, 10.1093/aob/mcw154, 2016.

Zhu, G. L., and Steudle, E.: Water Transport across Maize Roots, Simultaneous Measurement of Flows at the Cell and Root Level by Double Pressure Probe Technique, 95, 305-315, 10.1104/pp.95.1.305, 1991.

Zhu, S. G., Chen, H. S., Zhang, X. X., Wei, N., Wei, S. G., Yuan, H., Zhang, S. P., Wang, L. L., Zhou, L. H., and Dai, Y. J.: Incorporating root hydraulic redistribution and compensatory water uptake in the Common Land Model:

940   Effects on site level and global land modeling, J. Geophys. Res.-Atmos., 122, 7308-7322, 10.1002/2016jd025744, 2017.